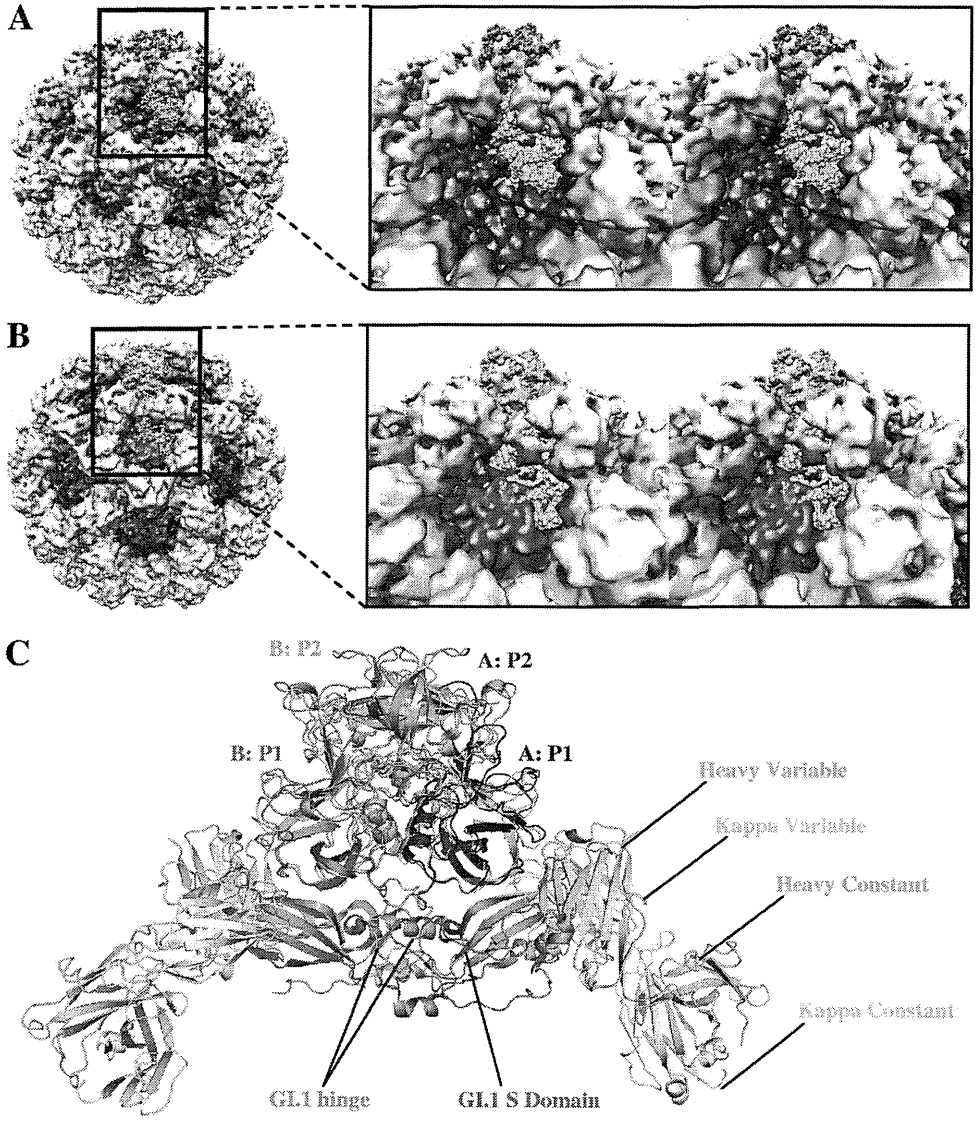

FIG 5 The X-ray crystal structure of the GII.10 P domain-Fab complex fitted into the cryo-EM structure of the GII.10 VLP and the X-ray crystal structure of the GI.1 VLP (PDB ID 1IHM). (A) The P domain (light blue and pink) from the P domain-Fab was fitted into the A/B dimer subunit on the VLP. The boxed region shows a close-up stereoview of the interaction. The Fab appeared to make slight contact with the S domain at the space at the 6-fold axes and was under a neighboring domain. (B) The P domain (cyan) from the P domain-Fab was fitted into the C/C dimer subunit on the VLP. The boxed region shows a close-up stereoview of the interaction. The Fab appeared to make contact with a raised S domain structure at the space at the 5-fold axes and was for the most part hidden under a neighboring domain. (C) The GII.10 P domain (colored as in Fig. 1 and rotated 90° from the views in Fig. 5A and 5B) was highly similar to the GI.1 P domain (light gray), but the Fabs clashed with the GI.1 S domain (orange).

used for fitting the GII.10 P domain-Fab complex and to describe the binding interaction in the context of the entire particle. The P domains of GI.1 and GII.10 matched well (root mean square deviation [RMSD], 1.3 Å), but the 5B18 Fab clashed with the GI.1 S domain (Fig. 5C). Indeed, the P domains in GI.1 VLPs rest on the S domains, and this necessarily placed most of the Fab structure into a position that overlapped the S domain (Fig. 5C). In an attempt to understand the 5B18 antibody interaction in the context of a GII VLP, the cryo-EM structure of the GII.10 VLP was determined to an ~10-Å resolution. Recent cryo-EM studies have shown that GI.1 and GV.1 norovirus capsid structures are strikingly different (30, 67), whereas another study indicated that GI.1 and GII.4 (Grimsby virus) capsids are highly similar (12). The cryo-EM structure of the GII.10 VLPs showed several structural similarities to the GV.1 virion, including a raised P domain, P1-P1 subdomain contacts, and an extended hinge region (see Fig. S6 in the supplemental material). In addition, the GII.10 and GV.1 P domain dimers were rotated ~40° clockwise compared to the orientation of the GI.1 P domain dimer (data not shown). Fitting of the X-ray crystal structure of the GII.10 P domain-Fab complex into the GII.10 VLP structure showed that the P domain could be positioned unambiguously into the P domain density of the EM map; however, this placement resulted in significant overlap between Fab and neighboring P and S domains in the virus particle (Fig. 5). One potential explanation for this result is that the VLPs flexibly expose the P domain to the 5B18 antibody by rotating the

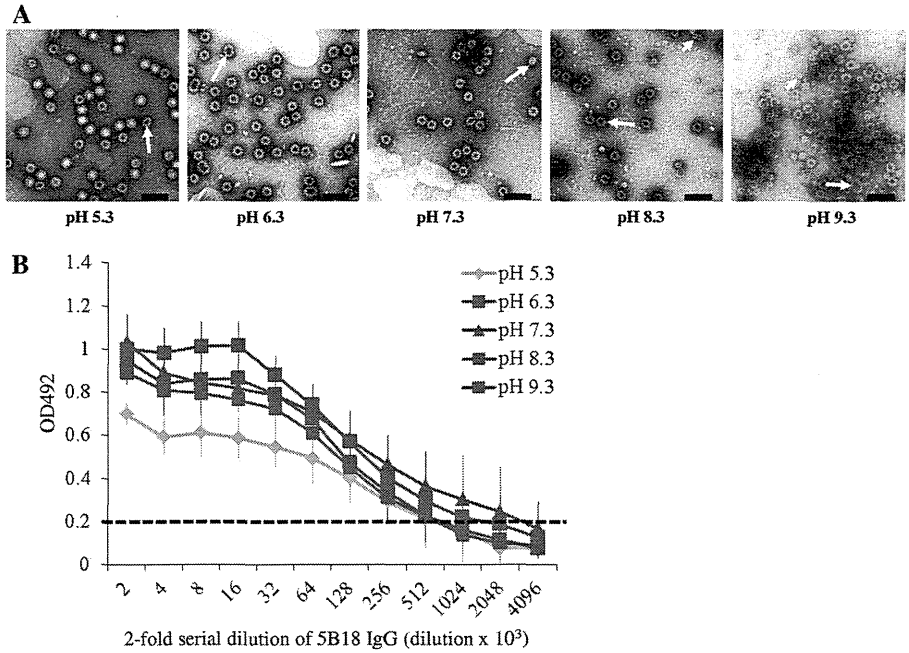

FIG 6 An antibody ELISA was used to determine the binding ability of IgG to GII.10 VLPs. (A) The morphology of the VLPs was examined using EM. At low pHs (from pH 5.3 to 7.3), the majority of the VLPs appeared intact, while above pH 7.3, many of the VLPs appeared broken (long arrows). Small VLPs were also found (short arrows). Scale bar, 100 nm. (B) The same VLPs shown in panel A were used in an ELISA to compare the binding ability of 5B18 IgG. The OD values represent the means of the results for 4 wells; error bars are shown. The OD at 492 nm (OD492) was determined; the dashed line shows the OD492 cutoff of 0.2 (21). The 5B18 IgG detected GII.10 VLPs at different pH values. At pH 7.3, the titer was 2,048,000, while the titers of the other pH values were 2- or 4-fold lower, indicating similar cross-reactivities.

P domains out of the conformation observed in the cryo-EM reconstruction and breaking the P1-P1 domain contacts seen in the VLP. This may be possible since the S domain-P1 subdomain connection in GII noroviruses is particularly long and flexible.

The structural differences between the GI.1 and GII.10 norovirus VLPs do not appear to be a consequence of sequence diversity, since the GI.1 and GII.4 VLP structures are similar and distinct from the GV.1 virion and GII.10 VLP structures. Moreover, the VLP preparation and cryo-EM techniques appear to be essentially the same (54). Two factors that may have affected the particle structures were the insect cell type and the pH of the VLPs. The GI.1 VLPs were expressed in *Spodoptera frugiperda* (Sf9) cells, purified by CsCl ultracentrifugation, and then resuspended in water (pH not described in text) (53, 54), and the GII.10 VLPs were expressed in *Trichopulsia ni* (H5) cells, purified by CsCl ultracentrifugation, and then resuspended in PBS (pH 7.3). We note parenthetically that the cryo-EM structures of hepatitis E virus VLPs expressed in Sf9 and H5 cells are similar, although the processing of the viral protein appeared different (38). Our EM results showed that GII.10 VLPs were intact particles at pH 5.3, 6.3, and 7.3, while another study found that the diameter of norovirus VLPs remained virtually unchanged at pH 3 to 7 but appeared smaller at pH 8 (2). This suggests that the insect cell line and water/PBS (neutral pH) did not affect the overall structure of the VLPs. However, another study has shown that a pH change from 7.6 to 5.0 could cause large structural changes in *Nudaurelia capensis* ω virus VLPs (43, 62). It is possible that these varied conformations do not represent different, stable norovirus structures but are rather all part of a wide spectrum of conformations afforded by the flexible tether between the P and S domains. From previous studies (30), it is clear that this "floating P domain" conformation is independent of whether the sample is a VLP or infectious virion. Since this extended conformation is now observed in rabbit hemorrhagic disease virus (also a calicivirus, genus *Lagovirus*), it also cannot be dependent upon calicivirus genera. It is possible that the energy differences between the conformations represented by these viruses is relatively small and that subtle protein-protein interaction differences favor one conformation under particular conditions. It would be particularly interesting to examine the conformations of these viruses under a broad range of conditions that mimic the expected environments during the viral life cycle. Such changes in virion structure have been observed with numerous other viruses (3, 9, 46, 64, 71). In the case of GV.1 norovirus, where there is an animal model (69) and infectious clone (66), it would also be important to determine what role this flexible tether region has in the replication of the virions and pathology of the disease.

It is important to note that the observed ELISA binding of 5B18 IgG may not occur with intact VLPs. It is possible that denatured or partially broken VLPs or the presence of contaminating GII.10 VP1 was responsible for the binding observed in the ELISA (19, 20, 24). However, it is known that high pH (8.3 or above), partially breaks or denatures norovirus VLPs (2). Despite this pH dependence, the titer remained almost identical, especially in the comparison between pHs 7.3 to 9.3 (Fig. 6), suggesting that only intact or structurally stable virions are being detected. Moreover, the 5B18 antibody could detect GII.10 VLPs that were bound to the plates via histo-blood group antigens, which required a dimeric interaction (22; also unpublished data). Finally three other antibodies, MAb14-1 and NV3901/NV3912, which bound in close

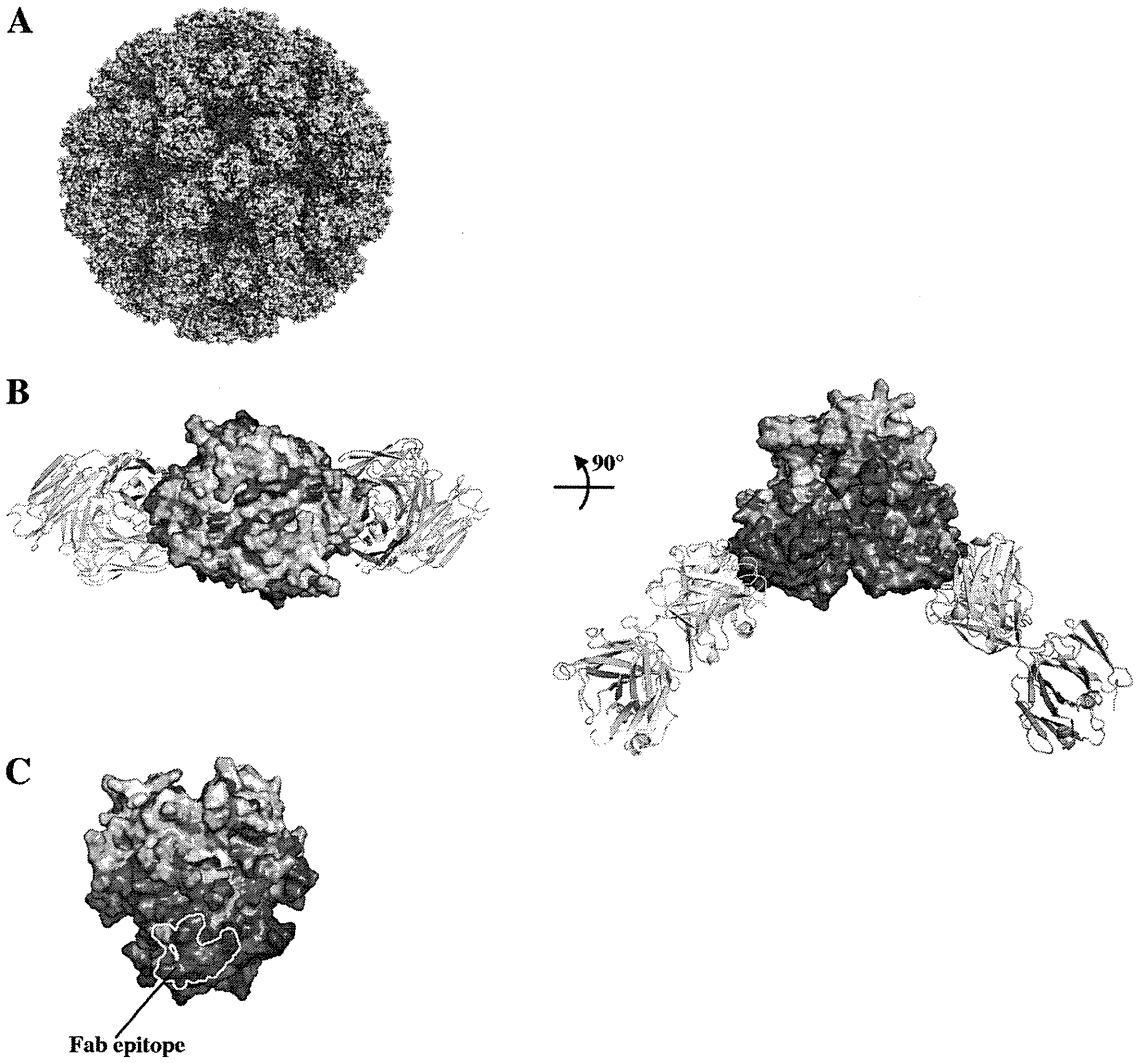

FIG 7 Surface representations of GII amino acid conservation. Noroviruses are genetically and antigenically distinct, with the S domain being more conserved than the P domain. (A) The GII amino acid variability was mapped onto the model of the GII.10 VLP (GI.1 S domain and GII.10 P domain). Amino acid conservation ranges are color-coded from deep purple (highly conserved) to white (highly variable). (B) The amino acid variability was mapped onto the GII.10 P domain apo structure (3ONU) with the 5B18 Fab bound. The top of the P domain was highly variable (left side), while the bottom half of the P domain was more conserved (right side). (C) The Fab binding footprint was mapped onto the P domain (yellow line). The footprint was at a highly conserved area on the wall of the P domain (inside the particle).

proximity to the 5B18 were all shown to detect VLPs (50, 59). These data therefore favor a model in which apparently intact norovirus capsids can indeed bind the 5B18 antibody (and other antibodies) despite significant steric clashes with the VLP structure.

Viruses often use remarkable conformational changes in their envelope or capsid structures to protect their genetic material by waiting for the proper cellular trigger to release their genome into the host cell. For example, the hemagglutinin spike in influenza undergoes a drastic pH-dependent conformational change in the endosome that initiates membrane fusion (8, 68). Similarly large pH-dependent changes have been observed with the enveloped flaviviruses (31, 32, 47) and alphaviruses (36, 45). Such changes due to environmental cues can expose or hide antigenic sites (e.g., see references 41, 45, and 47). Viruses can also receive cues via interactions with cellular receptors, as is the case with human rhinovirus (25, 26, 48). Viruses also undergo small, dynamic structural changes, "breathing" (6, 35, 37, 56), that are probably a prelude to the far larger conformational changes that occur during uncoating. These dynamic motions can transiently expose more-conserved antigenic sites that can be leveraged in designing vaccines (29, 37). However, the fact that these norovirus antibodies are recognizing deeply occluded portions of the P1 domain in apparently intact virions represents a different kind of viral dynamic: for this recognition to occur, the P domains must be capable of extremely large conformational changes without any obvious environmental cue. Such recognition would probably involve just one or a few P domains of a VLP being recognized by antibody 5B18; indeed, images of VLPs after incubation with an excess of antibody 5B18 for 1 h at 37°C (the same incubation used in the ELISA) shows them to be intact, with bound IgG difficult to detect (see Fig. S7 in the supplemental material).

Other antibodies have recently been described that bind to occluded sites on virions. With West Nile virus, the fusion loop-specific antibody E53 recognizes an epitope that should be inaccessible on mature virions. However, this antibody could neutralize mature West Nile virus in a time- and temperature-dependent manner, indicating a role of virus "breathing" or conformational dynamics in antibody recognition (17). With HIV-1, broadly neutralizing antibodies against the membrane-proximal external region of the virus do not appear to recognize the native viral spike (11, 58), again implicating conformational rearrangements to permit antibody recognition. These studies, along with the present study on norovirus recognition by 5B18, suggest substantial flexibility in certain virus particles as being important biologically for antibody-mediated recognition.

In summary, we have shown that a broadly reactive monoclonal antibody binds to an occluded site on the GII.10 P1 subdomain. The binding site was in close proximity to other monoclonal antibody binding sites, suggesting that the site contained an immunodominant region. We also found that the GII.10 VLP structure was more closely related to a GV.1 virion structure than to a GI.1 VLP structure and has marked flexibility in the P domains. These studies suggest that the P domain of noroviruses is capable of adopting variable conformations with respect to the S domain. Despite the vaunted diversity of noroviruses, especially on the exposed outer surface of the virion, one mechanism to achieve near pan-recognition by antibody may be to target a highly conserved domain interface that is dynamically exposed to the environment.

ACKNOWLEDGMENTS

We thank J. Stuckey for assistance with figures and members of the Structural Biology Section at the NIH Vaccine Research Center for help with Fab preparation and comments on the manuscript, K. Nagayama for generous help and insightful discussions, and M. Kataoka for assistance with electron microscopy.

G.S.H. and P.D.K. conceived the project; G.S.H. performed X-ray crystallography and biochemical assays with assistance from J.S.M., S.-Y.P., and P.D.K.; D.W.T. determined the cryo-EM structure with assistance from K.M.; M.Y., F.G., M.M., and K.K. provided the 5B18 IgG; I.G. mapped sequence conservation onto the GII.10 VLP; and G.S.H., D.W.T., J.S.M., T.J.S., I.G., J.R.H.T., K.M., and P.D.K. analyzed the data and wrote the paper, on which all authors commented.

Support for this work was provided by the Intramural Research Program of the National Institutes of Health (NIAID [P.D.K.]), USA, and by a Grant-in-Aid for Scientific Research, grants from the Ministry of Health, Labor, and Welfare of Japan, and a grant from the National Institute of Natural Sciences (NINS), Japan (K.M.). D.W.T is an NSF Graduate Research Fellow and performed this work in Japan as a JSPS/NSF East Asia and Pacific Summer Institute Fellow. Use of Sector 22 (Southeast Region Collaborative Access team) at the Advanced Photon Source was supported by the U.S. Department of Energy, Basic Energy Sciences, Office of Science, under contract no. W-31-109-Eng-38.

REFERENCES

1. **Adams PD, et al.** 2010. PHENIX: a comprehensive Python-based system for macromolecular structure solution. Acta Crystallogr. D. Biol. Crystallogr. **66**(Pt 2):213–221.
2. **Ausar SF, Foubert TR, Hudson MH, Vedvick TS, Middaugh CR.** 2006. Conformational stability and disassembly of Norwalk virus-like particles. Effect of pH and temperature. J. Biol. Chem. **281**:19478–19488.
3. **Belnap DM, et al.** 2000. Molecular tectonic model of virus structural transitions: the putative cell entry states of poliovirus. J. Virol. **74**:1342–1354.
4. **Bhella D, Gatherer D, Chaudhry Y, Pink R, Goodfellow IG.** 2008. Structural insights into calicivirus attachment and uncoating. J. Virol. **82**:8051–8058.
5. **Bhella D, Goodfellow IG.** 2011. The cryo-electron microscopy structure of feline calicivirus bound to junctional adhesion molecule A at 9-angstrom resolution reveals receptor-induced flexibility and two distinct conformational changes in the capsid protein VP1. J. Virol. **85**: 11381–11390.
6. **Bothner B, Dong XF, Bibbs L, Johnson JE, Siuzdak G.** 1998. Evidence of viral capsid dynamics using limited proteolysis and mass spectrometry. J. Biol. Chem. **273**:673–676.
7. **Bu W, et al.** 2008. Structural basis for the receptor binding specificity of Norwalk virus. J. Virol. **82**:5340–5347.
8. **Bullough PA, Hughson FM, Skehel JJ, Wiley DC.** 1994. Structure of influenza haemagglutinin at the pH of membrane fusion. Nature **371**: 37–43.
9. **Canady MA, Tihova M, Hanzlik TN, Johnson JE, Yeager M.** 2000. Large conformational changes in the maturation of a simple RNA virus, nudaurelia capensis omega virus (NomegaV). J. Mol. Biol. **299**:573–584.
10. **Cao S, et al.** 2007. Structural basis for the recognition of blood group trisaccharides by norovirus. J. Virol. **81**:5949–5957.
11. **Chakrabarti BK, et al.** 2011. Direct antibody access to the HIV-1 membrane-proximal external region positively correlates with neutralization sensitivity. J. Virol. **85**:8217–8226.
12. **Chen R, et al.** 2004. Inter- and intragenus structural variations in caliciviruses and their functional implications. J. Virol. **78**:6469–6479.
13. **Choi JM, Hutson AM, Estes MK, Prasad BV.** 2008. Atomic resolution structural characterization of recognition of histo-blood group antigens by Norwalk virus. Proc. Natl. Acad. Sci. U. S. A. **105**:9175–9180.
14. **Collaborative Computational Project N.** 1994. The CCP4 suite: programs for protein crystallography. Acta Crystallogr. D. Biol. Crystallogr. **50**:760–763.
15. **de Bruin E, Duizer E, Vennema H, Koopmans MP.** 2006. Diagnosis of Norovirus outbreaks by commercial ELISA or RT-PCR. J. Virol. Methods **137**:259–264.
16. **Dolinsky TJ, Nielsen JE, McCammon JA, Baker NA.** 2004. PDB2PQR: an automated pipeline for the setup of Poisson-Boltzmann electrostatics calculations. Nucleic Acids Res. **32**:W665–W667.
17. **Dowd KA, Jost CA, Durbin AP, Whitehead SS, Pierson TC.** 2011. A dynamic landscape for antibody binding modulates antibody-mediated neutralization of West Nile virus. PLoS Pathog. **7**:e1002111.
18. **Emsley P, Lohkamp B, Scott WG, Cowtan K.** 2010. Features and development of COOT. Acta Crystallogr. D. Biol. Crystallogr. **66**:486–501.
19. **Graham DY, et al.** 1994. Norwalk virus infection of volunteers: new insights based on improved assays. J. Infect. Dis. **170**:34–43.
20. **Greenberg HB, et al.** 1981. Proteins of Norwalk virus. J. Virol. **37**:994–999.
21. **Hansman GS, et al.** 2006. Genetic and antigenic diversity among noroviruses. J. Gen. Virol. **87**:909–919.
22. **Hansman GS, et al.** 2011. Crystal structures of GII.10 and GII.12 norovirus protruding domains in complex with histo-blood group antigens reveal details for a potential site of vulnerability. J. Virol. **85**:6687–6701.
23. **Hansman GS, et al.** 2004. Detection of norovirus and sapovirus infection among children with gastroenteritis in Ho Chi Minh City, Vietnam. Arch. Virol. **149**:1673–1688.
24. **Hardy ME, White LJ, Ball JM, Estes MK.** 1995. Specific proteolytic cleavage of recombinant Norwalk virus capsid protein. J. Virol. **69**:1693–1698.
25. **Hewat EA, Blaas D.** 2004. Cryoelectron microscopy analysis of the structural changes associated with human rhinovirus type 14 uncoating. J. Virol. **78**:2935–2942.
26. **Hoover-Litty H, Greve JM.** 1993. Formation of rhinovirus-soluble ICAM-1 complexes and conformational changes in the virion. J. Virol. **67**:390–397.
27. **Jiang X, Wang M, Graham DY, Estes MK.** 1992. Expression, self-assembly, and antigenicity of the Norwalk virus capsid protein. J. Virol. **66**:6527–6532.
28. **Kamata K, et al.** 2005. Expression and antigenicity of virus-like particles of norovirus and their application for detection of noroviruses in stool samples. J. Med. Virol. **76**:129–136.
29. **Katpally U, Fu T, Freed DC, Casimiro DR, Smith TJ.** 2009. Antibodies to the buried N-terminus of rhinovirus VP4 exhibit cross-serotypic neutralization. J. Virol. **83**:7040–7048.

30. **Katpally U, et al.** 2010. High-resolution cryo-electron microscopy structures of murine norovirus 1 and rabbit hemorrhagic disease virus reveal marked flexibility in the receptor binding domains. J. Virol. **84**:5836–5841.
31. **Kaufmann B, et al.** 2009. Capturing a flavivirus pre-fusion intermediate. PLoS Pathog. **5**:e1000672.
32. **Kaufmann B, et al.** 2006. West Nile virus in complex with the Fab fragment of a neutralizing monoclonal antibody. Proc. Natl. Acad. Sci. U. S. A. **103**:12400–12404.
33. **Krissinel E, Henrick K.** 2007. Inference of macromolecular assemblies from crystalline state. J. Mol. Biol. **372**:774–797.
34. **Kwong PD, et al.** 1999. Probability analysis of variational crystallization and its application to gp120, the exterior envelope glycoprotein of type 1 human immunodeficiency virus (HIV-1). J. Biol. Chem. **274**:4115–4123.
35. **Lewis JK, Bothner B, Smith TJ, Siuzdak G.** 1998. Antiviral agent blocks breathing of the common cold virus. Proc. Natl. Acad. Sci. U. S. A. **95**: 6774–6778.
36. **Li L, Jose J, Xiang Y, Kuhn RJ, Rossmann MG.** 2010. Structural changes of envelope proteins during alphavirus fusion. Nature **468**:705–708.
37. **Li Q, Yafal AG, Lee YMH, Hogle J, Chow M.** 1994. Poliovirus neutralization by antibodies to internal epitopes of VP4 and VP1 results from reversible exposure of the sequences at physiological temperatures. J. Virol. **68**:3965–3970.
38. **Li TC, et al.** 2005. Essential elements of the capsid protein for self-assembly into empty virus-like particles of hepatitis E virus. J. Virol. **79**: 12999–13006.
39. **Li X, Zhou R, Tian X, Li H, Zhou Z.** 2010. Characterization of a cross-reactive monoclonal antibody against Norovirus genogroups I, II, III and V. Virus Res. **151**:142–147.
40. **Lochridge VP, Jutila KL, Graff JW, Hardy ME.** 2005. Epitopes in the P2 domain of norovirus VP1 recognized by monoclonal antibodies that block cell interactions. J. Gen. Virol. **86**:2799–2806.
41. **Lok S-M, et al.** 2008. Binding of a neutralizing antibody to dengue virus alters the arrangement of surface glycoproteins. Nat. Struct. Mol. Biol. **15**:312–317.
42. **Majeed S, et al.** 2003. Enhancing protein crystallization through precipitant synergy. Structure **11**:1061–1070.
43. **Matsui T, Lander G, Johnson JE.** 2009. Characterization of large conformational changes and autoproteolysis in the maturation of a T=4 virus capsid. J. Virol. **83**:1126–1134.
44. **McCoy AJ, et al.** 2007. Phaser crystallographic software. J. Appl. Crystallogr. **40**:658–674.
45. **Meyer WJ, Gidwitz S, Ayers VK, Schoepp RJ, Johnston RE.** 1992. Conformational alteration of Sindbis virion glycoproteins induced by heat, reducing agents, or low pH. J. Virol. **66**:3504–3513.
46. **Miao Y, Johnson JE, Ortoleva PJ.** 2010. All-atom multiscale simulation of cowpea chlorotic mottle virus capsid swelling. J. Phys. Chem. B. **114**: 11181–11195.
47. **Modis Y, Ogata S, Clements D, Harrison SC.** 2004. Structure of the dengue virus envelope protein after membrane fusion. Nature **427**:313–319.
48. **Olson NH, et al.** 1993. Structure of a human rhinovirus complexed with its receptor molecule. Proc. Natl. Acad. Sci. U. S. A. **90**:507–511.
49. **Otwinowski Z, Minor W.** 1997. Processing of X-ray diffraction data collected in oscillation mode. Methods Enzymol. **276**:307–326.
50. **Parker TD, Kitamoto N, Tanaka T, Hutson AM, Estes MK.** 2005. Identification of genogroup I and genogroup II broadly reactive epitopes on the norovirus capsid. J. Virol. **79**:7402–7409.
51. **Pei J, Grishin NV.** 2001. AL2CO: calculation of positional conservation in a protein sequence alignment. Bioinformatics **17**:700–712.
52. **Pettersen EF, et al.** 2004. UCSF Chimera—a visualization system for exploratory research and analysis. J. Comput. Chem. **25**:1605–1612.
53. **Prasad BV, et al.** 1999. X-ray crystallographic structure of the Norwalk virus capsid. Science **286**:287–290.
54. **Prasad BV, Rothnagel R, Jiang X, Estes MK.** 1994. Three-dimensional structure of baculovirus-expressed Norwalk virus capsids. J. Virol. **68**: 5117–5125.
55. **Rabenau HF, et al.** 2003. Laboratory diagnosis of norovirus: which method is the best? Intervirology **46**:232–238.
56. **Reisdorph N, et al.** 2003. Human rhinovirus capsid dynamics is controlled by canyon flexibility. Virology **314**:34–44.
57. **Richards AF, et al.** 2003. Evaluation of a commercial ELISA for detecting Norwalk-like virus antigen in faeces. J. Clin. Virol. **26**:109–115.
58. **Ruprecht CR, et al.** 2011. MPER-specific antibodies induce gp120 shedding and irreversibly neutralize HIV-1. J. Exp. Med. **208**:439–454.
59. **Shiota T, et al.** 2007. Characterization of a broadly reactive monoclonal antibody against norovirus genogroups I and II: recognition of a novel conformational epitope. J. Virol. **81**:12298–12306.
60. **Tan M, Hegde RS, Jiang X.** 2004. The P domain of norovirus capsid protein forms dimer and binds to histo-blood group antigen receptors. J. Virol. **78**:6233–6242.
61. **Tang G, et al.** 2007. EMAN2: an extensible image processing suite for electron microscopy. J. Struct. Biol. **157**:38–46.
62. **Tang J, et al.** 2009. Dynamics and stability in maturation of a T=4 virus. J. Mol. Biol. **392**:803–812.
63. **Taube S, et al.** 2010. High-resolution X-ray structure and functional analysis of the murine norovirus 1 capsid protein protruding domain. J. Virol. **84**:5695–5705.
64. **Trus BL, et al.** 1996. The herpes simplex virus procapsid: structure, conformational changes upon maturation, and roles of the triplex proteins VP19c and VP23 in assembly. J. Mol. Biol. **263**:447–462.
65. **van Heel M, Harauz G, Orlova EV, Schmidt R, Schatz M.** 1996. A new generation of the IMAGIC image processing system. J. Struct. Biol. **116**: 17–24.
66. **Ward VK, et al.** 2007. Recovery of infectious murine norovirus using pol II-driven expression of full-length cDNA. Proc. Natl. Acad. Sci. U. S. A. **104**:11050–11055.
67. **Widdowson M-A, et al.** 2005. Detection of serum antibodies to bovine norovirus in veterinarians and the general population in the Netherlands. J. Med. Virol. **76**:119–128.
68. **Wilson IA, Skehel JJ, Wiley DC.** 1981. Structure of the haemagglutinin membrane glycoprotein of influenza virus at 3Å resolution. Nature **289**: 366–373.
69. **Wobus CE, Thackray LB, Virgin HW.** 2006. Murine norovirus: a model system to study norovirus biology and pathogenesis. J. Virol. **80**:5104–5112.
70. **Yoda T, et al.** 2003. Precise characterization of norovirus (Norwalk-like virus)-specific monoclonal antibodies with broad reactivity. J. Clin. Microbiol. **41**:2367–2371.
71. **Yu IM, et al.** 2008. Structure of the immature dengue virus at low pH primes proteolytic maturation. Science **319**:1834–1837.
72. **Zheng DP, et al.** 2006. Norovirus classification and proposed strain nomenclature. Virology **346**:312–323.

Arch Virol
DOI 10.1007/s00705-012-1387-7

BRIEF REPORT

A confirmation of sapovirus re-infection gastroenteritis cases with different genogroups and genetic shifts in the evolving sapovirus genotypes, 2002-2011

Seiya Harada · Tomoichiro Oka · Eisuke Tokuoka · Naoko Kiyota · Koichi Nishimura · Yasushi Shimada · Takehiko Ueno · Shigeru Ikezawa · Takaji Wakita · Qiuhong Wang · Linda J. Saif · Kazuhiko Katayama

Received: 10 April 2012 / Accepted: 12 May 2012

Abstract Sapovirus (SaV) is an important pathogen that causes acute gastroenteritis in humans. Human SaV is highly diverse genetically and is classified into multiple genogroups and genotypes. At present, there is no clear evidence for gastroenteritis cases caused by re-infection with SaV. We found that two individuals were sequentially infected with SaVs of two different genogroups and had gastroenteritis after each infection, although in one of the subsequent cases, both SaV and norovirus were detected. We also found a genetic shift in SaVs from gastroenteritis outpatients in the same geographical location. Our results suggest that protective immunity may be at least genogroup-specific for SaV.

Keywords Sapovirus · Gastroenteritis · Genotyping · Re-infection

Sapovirus (SaV), a member of the family *Caliciviridae*, is an important pathogen that causes acute gastroenteritis [1, 2, 5, 8, 10, 11, 13, 14, 20–25]. The SaV genome is a single-stranded 7.5-kb RNA molecule of positive polarity. SaV strains are highly diverse, especially in the capsid-encoding region [16], and are divided into at least five genogroups (GI to GV): Viruses belonging to GI, GII, GIV, and GV infect humans, and those belonging to GIII infect pigs [3, 18]. Based on the complete nucleotide sequences of the capsid gene, we have classified human SaVs into 16 genotypes (GI.1-7, GII.1-7, GIV, and GV)[18]. To date, there is no clear evidence for cases of gastroenteritis due to re-infection with SaV.

Previously, we identified 81 SaVs from outpatients with acute gastroenteritis in three pediatric clinics during 2002-2007 [8]. However, genotype analysis has not been performed with those samples. In this study, we detected 58 SaVs from the same clinics from 2008 to 2011 and genotyped all 139 SaVs isolated from 2002 to 2011. For the first time, we have identified cases of gastroenteritis due to re-infection with SaVs belonging to different genogroups. The GIV SaVs, which emerged in 2007, were not detected between 2008 and 2011, and the major genotype changed to GII.3 in 2008.

Stool specimens were collected from 728 patients with acute gastrointestinal symptoms at three pediatric clinics in Kumamoto Prefecture, Japan, from January 2008 to March 2011. Acute gastroenteritis was defined as a case in which

S. Harada and T. Oka contributed equally to this study.

S. Harada · E. Tokuoka · N. Kiyota · K. Nishimura
Kumamoto Prefectural Institute of Public Health and Environmental Science, Kumamoto, Japan

T. Oka (✉) · T. Wakita · K. Katayama
Department of Virology II, National Institute of Infectious Diseases, Gakuen 4-7-1, Musashi-murayama, Tokyo 208-0011, Japan
e-mail: oka-t@nih.go.jp

T. Oka · Q. Wang · L. J. Saif
Department of Veterinary Preventive Medicine, Food Animal Health Research Program, Ohio Agricultural Research and Development Center, The Ohio State University, Wooster, OH, USA

Y. Shimada
Shimada Children's Clinic, Kumamoto, Japan

T. Ueno
Ueno Pediatric Clinic, Kumamoto, Japan

S. Ikezawa
Ikezawa Children's Clinic, Kumamoto, Japan

Published online: 08 July 2012

the patient exhibits one or more of the following symptoms: vomiting, abdominal pain, and diarrhea. Specimens were collected during the symptomatic period, transported to the Kumamoto Prefectural Institute of Public Health and Environmental Science, and stored at −80°C until use. Viral nucleic acid extraction, cDNA synthesis, and PCR screening for SaV with the primers SaV124F, SaV1F, SaV5F, and SaV1245R[16] were performed as described [8]. For SaV-positive specimens, genogroup-specific PCR with primers SV-F13, SV-F14, SV-G1-R, SV-G2-R, SV-G4-R, and SV-G5-R [20] and nested PCR with primers SV-F13, SV-F14, SV-R13, and SV-R14 for the first PCR and with primers SV-F22 and SV-R2 or SV-F22, SV-R13, and SV-R14 for the second PCR [20] were performed as described [8]. PCR products corresponding to the partial SaV capsid-encoding region were purified and sequenced as described [8, 9]. SaV was detected in 58 (8.0 %) of 728 stool specimens collected from January 2008 to March 2011. All of these 58 specimens were successfully amplified in combination with a genogroup-specific PCR or nested PCR; 55 (94.8 %) and 54 (93.1 %) were positive by genogroup-specific PCR and nested PCR, respectively. These results demonstrate the efficiency of the SaV screening PCR assays used in this study. Nucleotide sequences for the 58 SaV strains that were newly detected during 2008 to 2011 were deposited in GenBank/EMBL/DDBJ under accession numbers AB689798-AB689855.

In total, 139 SaV strains were detected from 2002 to 2011 (81 sequenced in the previous study [8], and 58 newly identified and sequenced in this study) and were genotyped using phylogenetic analysis based on approximately 270 nucleotides of the partial capsid encoding region with reference strain sequences corresponding to the 16 genotypes (GI.1-7, GII.1-7, GIV, and GV) as described [18]. To investigate possible SaV re-infection cases, clinical records of the 139 SaV-positive patients were analyzed by the medical doctors of the three clinics. Stool specimens from the patients from whom SaVs were detected twice during the study period were further screened for enteric pathogens including norovirus (NoV), rotavirus, enteric adenovirus, astrovirus, kobuvirus, enterovirus, *Campylobacter*, *Escherichia coli* causing diarrhea, *Salmonella*, and *Shigella*. The sapovirus RNA load was determined by real-time PCR as described previously [8, 16].

As shown in Table 1, three children (patients A, B, and C) were positive for SaV twice during the study period. Patient A was positive for GI.1 SaV (1.50×10^9 copies/gram of stool) in January 2007, and GIV SaV (1.07×10^{11} copies/gram stool) in November 2007. Patient B was positive for GI.1 SaV (1.19×10^8 copies/gram stool) in December 2006, and both GII.3 SaV (1.00×10^6 copies/gram stool) and NoV GII (7.63×10^9 copies/gram stool) were detected in March 2009. Patient C was positive for GII.3 SaV (1.56×10^{11} copies/gram stool) at the first visit, and both GII.3 SaV (5.60×10^6 copies/gram stool) and GII NoV (5.05×10^9 copies/gram stool) were detected 18 days after the first visit (Table 1). Rotavirus, enteric adenovirus, astrovirus, kobuvirus, enterovirus, *Campylobacter, Escherichia coli* causing diarrhea, *Salmonella*, and *Shigella* were not detected in these three patients.

In this study, we detected at least two cases of re-infection with SaV of different genogroups 10 months (patient A) and 27 months (patient B) after their first visit to the clinic. Patient A was clearly a SaV re-infection gastroenteritis case, whereas SaV and/or NoV likely contributed to the diarrhea in the second visit in the case of

Table 1 Description of three gastroenteritis patients in whom sapovirus (SaV) was detected twice

Patient	Visit to clinic	Date of collection of stool specimen	SaV genotype	SaV copies/g stool[a]	Other pathogens[b]	NoV copies/g stool[c]	Clinical symptoms	Age	Sex
A	1st	2007 Jan 23	GI.1	1.50×10^9	–[d]	–[d]	Diarrhea, vomiting, abdominal pain	6 y 9 mo	F
	2nd	2007 Nov 20	GIV	1.07×10^{11}	–[d]	–[d]	Diarrhea, vomiting, abdominal pain		
B	1st	2006 Dec 14	GI.1	1.19×10^8	–[d]	–[d]	Diarrhea	2 y 7 mo	M
	2nd	2009 Mar 3	GII.3	1.00×10^6	NoV GII	7.63×10^9	Diarrhea		
C	1st	2008 Nov 7	GII.3	1.56×10^{11}	–[d]	–[d]	Bloody diarrhea	3 y 8 mo	F
	2nd	2008 Nov 25	GII.3	5.60×10^6	NoV GII	5.05×10^9	Vomiting		

[a] Quantitative SaV real-time RT-PCR was performed as described previously (ref 8, 16)

[b] Negative for rotavirus, enteric adenovirus, astrovirus, kobuvirus, enterovirus, *Campylobacter*, *Escherichia coli* causing diarrhea, *Salmonella*, and *Shigella*, tested as described previously (ref 8)

[c] Quantitative norovirus (NoV) real-time RT-PCR was performed as previously described (ref 8)

[d] Negative for NoV and other gastroenteritis pathogens tested as listed above

Table 2 Sapovirus genotypes in gastroenteritis outpatients at three pediatric clinics in the same area between June 2002 and March 2011

	Jan	Feb	Mar	Apr	May	Jun	Jul	Aug	Sep	Oct	Nov	Dec	Total number of SaV cases in each year
2002	NA	NA	NA	NA	NA							GI.1 (2)	2
2003		GI.1 (1) GII.1 (1) GII.2 (1)	GII.4 (1)	GII.2 (1)								GII.3 (2)	7
2004												GV (2)	2
2005	GI.1 (1)										GI.1 (1) GI.6 (1)	GI.1 (1) GI.6 (3)	7
2006									GI.1 (1)		GI.1 (1) GV (1)	GI.1 (4) GII.1 (3) GII.2 (1)	11
2007	GI.1 (1)								GIV(1)	GIV(11)	GIV (29)	GIV (10)	52
2008		**GII.7 (1)**		**GII.3 (1)** **GV (1)**	**GII.3 (2)**	**GII.3 (1)**				**GII.3 (1)**	**GII.3 (3)**	**GII.3 (1)**	**11**
2009	**GI.1 (1)** **GII.1 (1)** **GII.3 (1)**	**GI.3 (2)** **GII.1 (3)** **GII.3 (1)**	**GII.3 (5)**	**GI.1 (1)** **GII.3 (2)**	**GII.3 (1)**					**GII.3 (3)**	**GII.3 (1)**		**22**
2010		**GI.1 (1)**	**GI.1 (4)**	**GI.1 (4)** **GII.3 (1)**	**GI.2 (3)**	**GI.1 (1)** **GII.1 (1)**	**GII.2 (1)**				**GII.3 (2)**	**GI.1 (1)** **GII.1 (1)** **GII.3 (1)** **GV (1)**	**22**
2011			**GII.1 (2)** **GV (1)**	**NA**	**NA**	**NA**	**NA**	**NA**	**NA**	**NA**	**NA**	**NA**	**3**
Total numbers of SaV in each month	5	11	13	11	6	3	1	0	2	15	39	33	

The 58 strains detected from 2008 to 2011 are indicated in bold

Nucleotide sequences for the 81 SaV strains detected from 2002 to 2007 were deposited in GenBank/EMBL/DDBJ under accession numbers AB429079-AB429159 (ref 8)

Nucleotide sequences for the 58 SaV strains detected from 2008 to 2011 were deposited in GenBank/EMBL/DDBJ under accession numbers AB689798-AB689855

Genotype numbers are according to the classfication scheme of Oka et al. (ref 18)

The numbers detected are indicated in parentheses

NA no samples were available

patient B (Table 1). Patient C was probably not a SaV re-infection case, because SaV shedding can last for 1-4 weeks after gastroenteritis symptoms subside, as reported previously [11]. Indeed, the patient recovered from diarrhea but 18 days later had different symptoms (i.e., vomiting) (Table 1), and the two stool samples from patient C contained the same genotype of SaV with 99.0 % (606/ 612) nucleotide sequence identity within the partial capsid region (data not shown). Furthermore, the SaV RNA load from a stool specimen at the second visit was 4 $\log_{10}$ lower than that at the first visit, and high levels of GII NoV were detected at the second visit, coincident with the vomiting observed (Table 1). Thus, we conclude that the vomiting of patient C at the second visit was likely due to NoV infection.

Nakata et al. reported a significant rise in antibody levels after SaV infection, and serum anti-SaV antibody levels may correlate with resistance to SaV gastroenteritis [15]. However, our results suggest that protective immunity may be at least genogroup-specific for SaV or that protective immunity does not last for a long time. A follow-up survey can provide additional information to answer this question, because serum samples were not collected in our study.

The 139 SaV strains detected from 2002 to 2011 were classified into four genogroups and 11 genotypes: GI.1 (n=26), GI.2 (n=3), GI.3 (n=2), GI.6 (n=4), GII.1 (n=12), GII.2 (n=4), GII.3 (n=29), GII.4 (n=1), GII.7 (n=1), GIV (n=51) and GV (n=6) (Table 2). GIV SaVs were predominant in 2007, as reported previously [8], but they were not detected in 2008-2011. Instead, GII.3 SaVs became predominant in 2008 and then gradually decreased in 2009 and 2010 (Table 2). The SaV capsid-encoding region is highly diverse among different genogroups/genotypes at both the nucleic acid and amino acid sequence level [3, 7, 18, 19], and SaV strains of different genogroups and genotypes have distinct antigenicities [4, 6, 7, 12, 17]. Such genogroup/genotype shifts of SaVs in the population in the same geographic area may be due to herd immunity, although further study is required to assess this.

In conclusion, we found SaV re-infection gastroenteritis case(s) for the first time. Our data indicate that people can be sequentially infected with SaVs of different genogroups during their life and that they may suffer from gastroenteritis after each infection, as was clearly evident for patient A. We also found a genetic shift in SaV among the gastroenteritis outpatients in the same restricted geographical location. Global SaV surveillance and seroprevalence studies are warranted to investigate whether such re-infections and genetic shifts occur in other geographic areas and whether SaV protective immunity is genogroup/genotype-specific.

Acknowledgments This work was supported in part by a grant for Research on Emerging and Re-emerging Infectious Diseases from the Ministry of Health, Labour, and Welfare of Japan.

References

1. Cheng WX, Ye XH, Yang XM, Li YN, Jin M, Jin Y, Duan ZJ (2010) Epidemiological study of human calicivirus infection in children with gastroenteritis in Lanzhou from 2001 to 2007. Arch Virol 155:553–555
2. Chiba S, Nakata S, Numata-Kinoshita K, Honma S (2000) Sapporo virus: history and recent findings. J Infect Dis 181(Suppl 2): S303–S308
3. Farkas T, Zhong WM, Jing Y, Huang PW, Espinosa SM, Martinez N, Morrow AL, Ruiz-Palacios GM, Pickering LK, Jiang X (2004) Genetic diversity among sapoviruses. Arch Virol 149: 1309–1323
4. Farkas T, Deng X, Ruiz-Palacios G, Morrow A, Jiang X (2006) Development of an enzyme immunoassay for detection of sapovirus-specific antibodies and its application in a study of seroprevalence in children. J Clin Microbiol 44:3674–3679
5. Gallimore CI, Iturriza-Gomara M, Lewis D, Cubitt D, Cotterill H, Gray JJ (2006) Characterization of sapoviruses collected in the United Kingdom from 1989 to 2004. J Med Virol 78:673–682
6. Hansman GS, Natori K, Oka T, Ogawa S, Tanaka K, Nagata N, Ushijima H, Takeda N, Katayama K (2005) Cross-reactivity among sapovirus recombinant capsid proteins. Arch Virol 150: 21–36
7. Hansman GS, Oka T, Sakon N, Takeda N (2007) Antigenic diversity of human sapoviruses. Emerg Infect Dis 13:1519–1525
8. Harada S, Okada M, Yahiro S, Nishimura K, Matsuo S, Miyasaka J, Nakashima R, Shimada Y, Ueno T, Ikezawa S, Shinozaki K, Katayama K, Wakita T, Takeda N, Oka T (2009) Surveillance of pathogens in outpatients with gastroenteritis and characterization of sapovirus strains between 2002 and 2007 in Kumamoto Prefecture, Japan. J Med Virol 81:1117–1127
9. Iizuka S, Oka T, Tabara K, Omura T, Katayama K, Takeda N, Noda M (2010) Detection of sapoviruses and noroviruses in an outbreak of gastroenteritis linked genetically to shellfish. J Med Virol 82:1247–1254
10. Iturriza-Gomara M, Elliot AJ, Dockery C, Fleming DM, Gray JJ (2009) Structured surveillance of infectious intestinal disease in pre-school children in the community: 'The Nappy Study'. Epidemiol Infect 137:922–931
11. Iwakiri A, Ganmyo H, Yamamoto S, Otao K, Mikasa M, Kizoe S, Katayama K, Wakita T, Takeda N, Oka T (2009) Quantitative analysis of fecal sapovirus shedding: identification of nucleotide substitutions in the capsid protein during prolonged excretion. Arch Virol 154:689–693
12. Jiang X, Cubitt WD, Berke T, Zhong W, Dai X, Nakata S, Pickering LK, Matson DO (1997) Sapporo-like human caliciviruses are genetically and antigenically diverse. Arch Virol 142: 1813–1827
13. Johansson PJ, Bergentoft K, Larsson PA, Magnusson G, Widell A, Thorhagen M, Hedlund KO (2005) A nosocomial sapovirus-associated outbreak of gastroenteritis in adults. Scand J Infect Dis 37:200–204
14. Mayo MA (2002) A summary of taxonomic changes recently approved by ICTV. Arch Virol 147:1655–1663
15. Nakata S, Chiba S, Terashima H, Yokoyama T, Nakao T (1985) Humoral immunity in infants with gastroenteritis caused by human calicivirus. J Infect Dis 152:274–279
16. Oka T, Katayama K, Hansman GS, Kageyama T, Ogawa S, Wu FT, White PA, Takeda N (2006) Detection of human sapovirus by

real-time reverse transcription-polymerase chain reaction. J Med Virol 78:1347–1353
17. Oka T, Miyashita K, Katayama K, Wakita T, Takeda N (2009) Distinct genotype and antigenicity among genogroup II sapoviruses. Microbiol Immunol 53:417–420
18. Oka T, Mori K, Iritani N, Harada S, Ueki Y, Iizuka S, Mise K, Murakami K, Wakita T, Katayama K (2012) Human sapovirus classification based on complete capsid nucleotide sequences. Arch Virol 157:349–352
19. Okada M, Yamashita Y, Oseto M, Ogawa T, Kaiho I, Shinozaki K (2006) Genetic variability in the sapovirus capsid protein. Virus Genes 33:157–161
20. Okada M, Yamashita Y, Oseto M, Shinozaki K (2006) The detection of human sapoviruses with universal and genogroup-specific primers. Arch Virol 151:2503–2509
21. Pang XL, Lee BE, Tyrrell GJ, Preiksaitis JK (2009) Epidemiology and genotype analysis of sapovirus associated with gastroenteritis outbreaks in Alberta, Canada: 2004–2007. J Infect Dis 199:547–551
22. Phan TG, Okame M, Nguyen TA, Maneekarn N, Nishio O, Okitsu S, Ushijima H (2004) Human astrovirus, norovirus (GI, GII), and sapovirus infections in Pakistani children with diarrhea. J Med Virol 73:256–261
23. Sdiri-Loulizi K, Hassine M, Gharbi-Khelifi H, Aouni Z, Chouchane S, Sakly N, Neji-Guediche M, Pothier P, Ambert-Balay K, Aouni M (2011) Molecular detection of genogroup I sapovirus in Tunisian children suffering from acute gastroenteritis. Virus Genes 43:6–12
24. Svraka S, Vennema H, van der Veer B, Hedlund KO, Thorhagen M, Siebenga J, Duizer E, Koopmans M (2010) Epidemiology and genotype analysis of emerging sapovirus-associated infections across Europe. J Clin Microbiol 48:2191–2198
25. Yoshida T, Kasuo S, Azegami Y, Uchiyama Y, Satsumabayashi K, Shiraishi T, Katayama K, Wakita T, Takeda N, Oka T (2009) Characterization of sapoviruses detected in gastroenteritis outbreaks and identification of asymptomatic adults with high viral load. J Clin Virol 45:67–71

Arch Virol (2012) 157:349–352
DOI 10.1007/s00705-011-1161-2

BRIEF REPORT

Human sapovirus classification based on complete capsid nucleotide sequences

Tomoichiro Oka · Kohji Mori · Nobuhiro Iritani · Seiya Harada · You Ueki · Setsuko Iizuka · Keiji Mise · Kosuke Murakami · Takaji Wakita · Kazuhiko Katayama

Received: 19 August 2011 / Accepted: 7 October 2011 / Published online: 11 November 2011

Abstract The genetically diverse sapoviruses (SaVs) are a significant cause of acute human gastroenteritis. Human SaV surveillance is becoming more critical, and a better understanding of the diversity and distribution of the viral genotypes is needed. In this study, we analyzed 106 complete human SaV capsid nucleotide sequences to provide a better understanding of their diversity. Based on those results, we propose a novel standardized classification scheme that meets the requirements of the International Calicivirus Scientific Committee. We believe the classification scheme and strains described here will be of value for the molecular characterization and classification of newly detected SaV genotypes and for comparing data worldwide.

Sapoviruses (SaVs) cause gastroenteritis in humans and are a significant public-health problem. Numerous studies have documented their importance in outbreaks of sporadic gastroenteritis and in contaminated food destined for human consumption [1, 3, 7, 8, 10–12, 16–19, 21, 23].

The SaV genome is a positive-sense, nonsegmented single-strand RNA molecule of approximately 7.5 kb that is polyadenylated at the 3′ terminus. The SaV genome contains two or three open reading frames (ORFs). ORF1 encodes non-structural proteins (i.e., VPg, protease, and RNA-dependent RNA polymerase [RdRp]) and a capsid protein (VP1). ORF2 and ORF3 encode proteins of unknown function. The capsid protein is thought to contain all of the determinants for viral attachment and antigenicity [2, 5].

The most widely used method of human SaV detection is reverse transcription–PCR (RT-PCR). It has high sensitivity and can be used to analyze the virus genetically [9, 16, 17, 20, 22]. Real-time RT-PCR is also used to detect the virus. It is highly sensitive and useful for quantitative analysis [14]. Direct serotyping based on neutralization is not possible for human SaVs because no cell-culture system supporting SaV replication has been established.

T. Oka (✉) · K. Murakami · T. Wakita · K. Katayama
Department of Virology II, National Institute of Infectious Diseases, Gakuen 4-7-1, Musashimurayama-shi, Tokyo 208-0011, Japan
e-mail: oka-t@nih.go.jp

T. Oka
Food Animal Health Research Program, Ohio Agricultural Research and Development Center, Department of Veterinary Preventive Medicine, The Ohio State University, Wooster, OH 44691, USA

K. Mori
Tokyo Metropolitan Institute of Public Health, Tokyo, Japan

N. Iritani
Osaka City Institute of Public Health and Environmental Sciences, Osaka, Japan

S. Harada
Kumamoto Prefectural Institute of Public Health and Environmental Science, Kumamoto, Japan

Y. Ueki
Miyagi Prefectural Institute of Public Health and Environment, Miyagi, Japan

S. Iizuka
Shimane Prefectural Institute of Public Health and Environmental Science, Shimane, Japan

K. Mise
Sapporo Medical University Center for Medical Education, Hokkaido, Japan

From the sequence data for complete capsids, human SaVs are a genetically diverse group [4]. At least four different human SaV genogroups and numerous genotypes have been described, and for the most part, the antigenicity corresponds well to the genetic classification [6, 15]. However, many molecular epidemiological studies have relied on only partially sequenced genes because the broadly reactive RT-PCR primer sets for the SaV capsid-encoding region were directed against highly conserved regions [16, 17, 22]. The International Calicivirus Scientific Committee at the Fourth International Conference on Caliciviruses in Chile (in 2010) proposed that new norovirus and SaV genotypes should only be named after the complete capsid sequence (approximately 1700 nt in length) is determined and compared to other complete capsid sequences. A standardized genotyping and nomenclature system based on appropriate criteria is necessary to facilitate worldwide comparison of data.

In this study, we have analyzed the nucleotide sequences of 107 complete SaV capsids (106 human SaVs and one porcine SaV). Ninety-one human SaV and one porcine SaV sequences were collected from the calicivirus database (http://teine.cc.sapmed.ac.jp/~calici/ddbj/) on February 23, 2011. The sequences of 16 additional human SaVs from gastroenteritis patients in five prefectures of Japan were newly determined by PCR-based direct sequencing as described [11, 12] and deposited in the DDBJ/Genbank/EMBL database under the following accession numbers: AB429084, AB522390–AB522392, AB622429, AB622432, AB622435–AB622439, AB622441, AB623037, AB630067, AB630068, and AB630340. The nucleic acid sequences were aligned with ClustalW (version 1.83), and the gaps were removed. The genetic distances were calculated using the Kimura's two-parameter method, and a distance matrix file was created (http://clustalw.ddbj.nig.ac.jp/top-j.html). These data were used to generate histograms of the relative frequency distributions of pairwise distance values (Graph Pad Prism version 4.0). The phylogenetic tree with 1000 bootstrap replicates was generated by the neighbor-joining (NJ) method using Clustal W (version 1.83) and was drawn with NJplot software (http://pbil.univ-lyon1.fr/software/njplot.html).

The frequency histogram of pairwise distance values with 107 SaV complete capsid nucleotide sequences resulted in three clearly distinct and non-overlapping symmetrical peaks (0–0.112 [mean 0.036], 0.153–0.414 [mean 0.290], and 0.606–0.872 [mean 0.683]) (Fig. 1). These three peaks were considered to represent the strain, genotype, and genogroup, respectively. The mean ± 3SD of each pairwise distance value for strain, genotype, and genogroup were 0–0.127, 0.201–0.379, and 0.562–0.803, respectively (Fig. 1). The cutoff values for the genotype and genogroup clusters were <0.200 and <0.561, respectively. A phylogenetic tree of the 107 SaV complete capsid nucleotide sequences was constructed by the NJ method (Fig. 2). SaV was divided into five genogroups, GI, GII, GIII, GIV, and GV, among which human SaV were classified into GI, GII, GIV, and GV. SaV GI and GII were each subdivided into seven genotypes, and GIV and GV were placed into a single genotype by the distance criteria as described above. The genotype numbers were assigned consecutively as shown in Fig. 2.

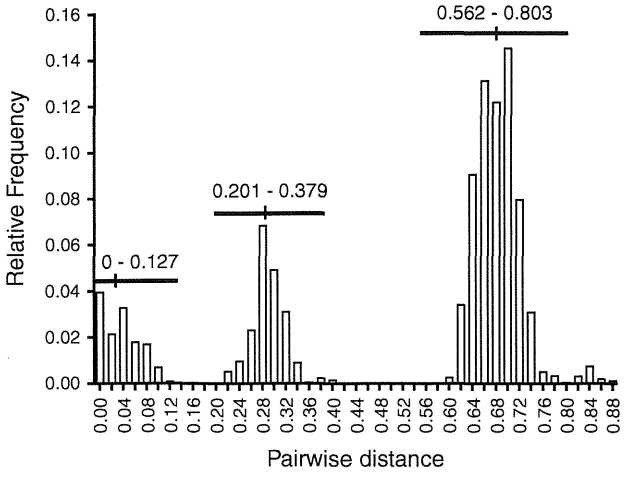

Fig. 1 Pairwise distance distribution of 107 SaV strains using the entire capsid nucleotide sequences. The horizontal bars indicates the mean value ± 3 SD for each distribution peaks of strain, genotype, and genogroup, respectively

Recent experiments with virus-like particles (VLPs) have demonstrated the different antigenicities among the GI, GII, GIV, and GV strains [6], and between GI.1 vs GI.5 [6, 7], and GII.2 vs GII.3 strains [15]. Therefore, a classification scheme based on the complete capsid sequence might well reflect the antigenic phenotype of SaV and can also be useful for selecting representative strains for preparing VLPs or VP1 panels for further immunological studies.

In conclusion, we provide a novel human SaV classification based on complete capsid gene sequences. Our classification scheme is based on statistically defined cutoff pairwise distance values. This classification method will aid in the molecular characterization and classification of newly detected SaV genotypes. Recently, a web-based automated genotyping tool for noroviruses was established by the National Institute for Public Health and the Environment and Centers for Disease Control and Prevention [13]. As the number of SaV surveillance laboratories appears to be increasing, a similar web-based genotyping tool with the reference nucleotide sequence sets described in this study will also be valuable for SaV data comparison.

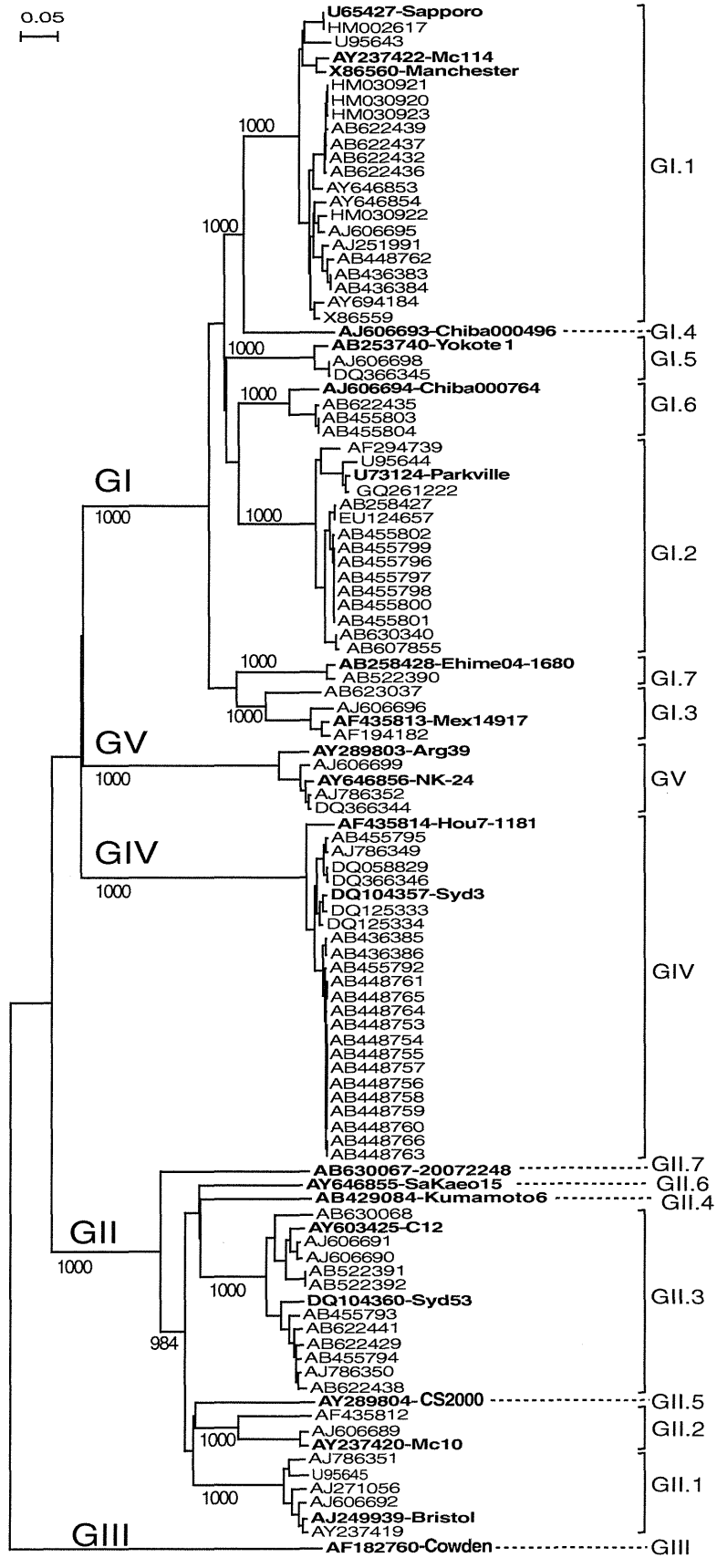

Fig. 2 Phylogenetic trees constructed using the entire capsid nucleotide sequences of 107 SaV strains. The accession numbers and assigned genogroup and genotypes are indicated. Representative strain(s) of each genogroup or genotype are indicated in boldface type. The bootstrap values correspond to 1000 replications. The number on each branch indicates the bootstrap value, where a value higher than 950 is indicated. The scale represents nucleotide substitutions per site

Acknowledgments This work was supported in part by grants for Research on Emerging and Re-emerging Infectious Diseases, as well as Research on Food Safety, from the Ministry of Health, Labour, and Welfare of Japan. We thank Mineyuki Okada for his assistance in sequencing and database submission.

References

1. Akihara S, Phan TG, Nguyen TA, Yagyu F, Okitsu S, Muller WE, Ushijima H (2005) Identification of sapovirus infection among Japanese infants in a day care center. J Med Virol 77:595–601
2. Clarke IN, Lambden PR (2000) Organization and expression of calicivirus genes. J Infect Dis 181(Supp 2):S309–S316
3. Dey SK, Phan TG, Nguyen TA, Nishio O, Salim AF, Yagyu F, Okitsu S, Ushijima H (2007) Prevalence of sapovirus infection among infants and children with acute gastroenteritis in Dhaka City, Bangladesh during 2004–2005. J Med Virol 79:633–638
4. Farkas T, Zhong WM, Jing Y, Huang PW, Espinosa SM, Martinez N, Morrow AL, Ruiz-Palacios GM, Pickering LK, Jiang X (2004) Genetic diversity among sapoviruses. Arch Virol 149: 1309–1323
5. Green KY (2007) Caliciviridae: the Noroviruses. In: Knipe DM, Howley PM, Griffin DE, Lamb RA, Martin MA, Roizman B, Straus SE (eds) Fields Virology, 5th edn. Lippincott Williams & Wilkins, Philadelphia, pp 949–979
6. Hansman GS, Oka T, Sakon N, Takeda N (2007) Antigenic diversity of human sapoviruses. Emerg Infect Dis 13:1519–1525
7. Hansman GS, Saito H, Shibata C, Ishizuka S, Oseto M, Oka T, Takeda N (2007) Outbreak of gastroenteritis due to sapovirus. J Clin Microbiol 45:1347–1349
8. Harada S, Okada M, Yahiro S, Nishimura K, Matsuo S, Miyasaka J, Nakashima R, Shimada Y, Ueno T, Ikezawa S, Shinozaki K, Katayama K, Wakita T, Takeda N, Oka T (2009) Surveillance of pathogens in outpatients with gastroenteritis and characterization of sapovirus strains between 2002 and 2007 in Kumamoto Prefecture, Japan. J Med Virol 81:1117–1127
9. Honma S, Nakata S, Sakai Y, Tatsumi M, Numata-Kinoshita K, Chiba S (2001) Sensitive detection and differentiation of Sapporo virus, a member of the family Caliciviridae, by standard and booster nested polymerase chain reaction. J Med Virol 65: 413–417
10. Iizuka S, Oka T, Tabara K, Omura T, Katayama K, Takeda N, Noda M (2010) Detection of sapoviruses and noroviruses in an outbreak of gastroenteritis linked genetically to shellfish. J Med Virol 82:1247–1254
11. Ishida S, Yoshizumi S, Miyoshi M, Ikeda T, Okui T, Katayama K, Takeda N, Oka T (2008) Characterization of sapoviruses detected in Hokkaido, Japan. Jpn J Infect Dis 61:504–506
12. Iwakiri A, Ganmyo H, Yamamoto S, Otao K, Mikasa M, Kizoe S, Katayama K, Wakita T, Takeda N, Oka T (2009) Quantitative analysis of fecal sapovirus shedding: identification of nucleotide substitutions in the capsid protein during prolonged excretion. Arch Virol 154:689–693
13. Kroneman A, Vennema H, Deforche K, v d Avoort H, Penaranda S, Oberste MS, Vinje J, Koopmans M (2011) An automated genotyping tool for enteroviruses and noroviruses. J Clin Virol 51:121–125
14. Oka T, Katayama K, Hansman GS, Kageyama T, Ogawa S, Wu FT, White PA, Takeda N (2006) Detection of human sapovirus by real-time reverse transcription-polymerase chain reaction. J Med Virol 78:1347–1353
15. Oka T, Miyashita K, Katayama K, Wakita T, Takeda N (2009) Distinct genotype and antigenicity among genogroup II sapoviruses. Microbiol Immunol 53:417–420
16. Okada M, Shinozaki K, Ogawa T, Kaiho I (2002) Molecular epidemiology and phylogenetic analysis of Sapporo-like viruses. Arch Virol 147:1445–1451
17. Okada M, Yamashita Y, Oseto M, Shinozaki K (2006) The detection of human sapoviruses with universal and genogroup-specific primers. Arch Virol 151:2503–2509
18. Pang XL, Lee BE, Tyrrell GJ, Preiksaitis JK (2009) Epidemiology and genotype analysis of sapovirus associated with gastroenteritis outbreaks in Alberta, Canada: 2004–2007. J Infect Dis 199:547–551
19. Svraka S, Vennema H, van der Veer B, Hedlund KO, Thorhagen M, Siebenga J, Duizer E, Koopmans M (2010) Epidemiology and genotype analysis of emerging sapovirus-associated infections across Europe. J Clin Microbiol 48:2191–2198
20. Vinje J, Deijl H, van der Heide R, Lewis D, Hedlund KO, Svensson L, Koopmans MP (2000) Molecular detection and epidemiology of Sapporo-like viruses. J Clin Microbiol 38:530–536
21. Yamashita Y, Ootsuka Y, Kondo R, Oseto M, Doi M, Miyamoto T, Ueda T, Kondo H, Tanaka T, Wakita T, Katayama K, Takeda N, Oka T (2010) Molecular characterization of Sapovirus detected in a gastroenteritis outbreak at a wedding hall. J Med Virol 82:720–726
22. Yan H, Yagyu F, Okitsu S, Nishio O, Ushijima H (2003) Detection of norovirus (GI, GII), Sapovirus and astrovirus in fecal samples using reverse transcription single-round multiplex PCR. J Virol Methods 114:37–44
23. Yoshida T, Kasuo S, Azegami Y, Uchiyama Y, Satsumabayashi K, Shiraishi T, Katayama K, Wakita T, Takeda N, Oka T (2009) Characterization of sapoviruses detected in gastroenteritis outbreaks and identification of asymptomatic adults with high viral load. J Clin Virol 45:67–71

frontiers in
MICROBIOLOGY

PERSPECTIVE ARTICLE
published: 06 November 2012
doi: 10.3389/fmicb.2012.00387

In silico 3D structure analysis accelerates the solution of a real viral structure and antibodies docking mechanism

Motohiro Miki*[1,2] *and Kazuhiko Katayama*[1]*

[1] *Department of Virology II, National Institute of Infectious Diseases, Tokyo, Japan*
[2] *Denka-Seiken Co., Ltd, Niigata, Japan*

Edited by:
Hironori Sato, National Institute of Infectious Diseases, Japan

Reviewed by:
Masaru Yokoyama, National Institute of Infectious Diseases, Japan
Sam-Yong Park, Yokohama City University, Japan

****Correspondence:***
Kazuhiko Katayama, Department of Virology II, National Institute of Infectious Diseases, Tokyo 208-0011, Japan.
e-mail: katayama@nih.go.jp

Norwalk virus (NoV) is responsible for most outbreaks of non-bacterial gastroenteritis. NoV is genetically diverse and show antigenically variable. Recently, we produced a monoclonal antibody called 5B-18 that reacts broadly with NoV genogroup II (GII). We suspected the 5B-18 binds to a conformational epitope on 3D structure of virion. X-ray crystallography showed us that 5B-18 binds to NoV at the P domain, which protrudes from the capsid surface of the virion. However, there seems to be no space that would allow the IgG to approach the virion. To solve this problem, we used cryo-electron microscopy to examine NoV GII virus-like particles (VLPs). The P domain rises up higher in NoV GII than in NoV GI, and it seems to form an outer layer around the virion. Finally, using *in silico* modeling we found the 5B-18 Fab arms and NoV P region are quite flexible, so that 5B-18 can bind the NoV virion from bottom of P domain. This study demonstrates the shortcomings of studying biological phenomenon by only one technique. Each method has limitations. Multiple methods and modeling *in silico* are the keys to solving structural problems.

Keywords: Norwalk virus, monoclonal antibody, x-ray crystallography, *in silico* modeling, cryo-electron microscopy

THE BASICS OF NORWALK VIRUS

Norwalk virus (NoV) is responsible for most of the outbreaks of non-bacterial gastroenteritis in developed countries and, it is thought, in developing countries as well. Yet, although NoV was identified more than 30 years ago, we know little about their pathogenicity and basic virology (Guix et al., 2007). Studies of NoV have been hampered by the lack of a cell-culture system or a small animal model in which the virus will grow, except murine norovirus that is classified as NoV genogroup V (Wobus et al., 2006).

NoV belongs to the family Caliciviridae. The genus *Norovirus* has only one species, *Norwalk viruses*, with five genogroups (GI–GV). Genogroup GI and II cause most human infections, and they are further subdivided into numerous genotypes (GI.1–8 and GII.1–17; Zheng et al., 2006). The NoV genome is a 7.3 to 7.7-kb positive-sense, polyadenylated, single-stranded RNA molecule. It contains three open reading frames (ORFs): ORF1 encodes a non-structural polyprotein, and ORF2 and ORF3 encode the major and minor capsid proteins, VP1 and VP2, respectively (Jiang et al., 1992; Lambden et al., 1993).

Without an *in vitro* system for propagating the virus, the antigenicity of NoV has been inferred from studies of virus-like particles (VLPs). Nucleic acid-free VLPs self-assemble when the capsid protein is expressed in a baculovirus expression system (**Figure 1A**). The VLPs are assumed to have a similar morphology and, thus, antigenicity as that of the native virions (Jiang et al., 1992). Cryo-electron microscopy (cryo-EM) and x-ray crystal structures of the prototype norovirus VLP (GI.1, Norwalk virus) showed that the VLPs form a T = 3 icosahedral structure (Prasad et al., 1994, 1999).

However, structures of large protein complexes are difficult to determine by x-ray analysis. We sought to understand the structure of the virion and how it interacts with antibodies by combining data from x-ray diffraction, cryo-EM, and *in silico* modeling.

A MONOCLONAL ANTIBODY REACTS BROADLY WITH NoV GII

NoV is generally detected by RT-PCR with degenerate primers or an ELISA with NoV-specific antibodies. Many polyclonal and monoclonal antibodies used in the ELISA kits were developed in mice or rabbit immunized with norovirus VLPs (Hansman et al., 2011).

Recently, we produced a monoclonal antibody called 5B-18 that reacts broadly with NoV GII (Hansman et al., 2012). In fact, 5B-18 is used as a NoV GII broad-range capture antibody in a commercial ELISA kit [NV-AD(III) SEIKEN NoV antigen ELISA] and in an immunochromatography (IC) kit (Quick naviNoro IC kit, both from Denka-Seiken, Japan).

The 5B-18 monoclonal antibody was produced by immunizing a mouse with norovirus VLPs. Several monoclonal antibodies bind to the shell (S) domain (Yoda et al., 2003; Li et al., 2010), and others bind to the protruding (P) domain (Lindesmith et al., 2012). We suspect that 5B-18 also binds to S or P domain on the surface of the NoV virion. However, no high-resolution structural details of the antibody binding to the VLPs, S domain or P domain are available.

X-RAY CRYSTALLOGRAPHY OF THE BINDING SITE

The 5B-18 binds major NoV genotypes, such as GII.4 and GII.3, and the minor NoV genotypes GII.10 and GII.12 strongly. We suspect 5B-18 binds to a conserved epitope on the NoV capsid surface. We wanted to define the recognition site of 5B-18 and the NoV minor genotype GII.10 P domain, and we began with x-ray

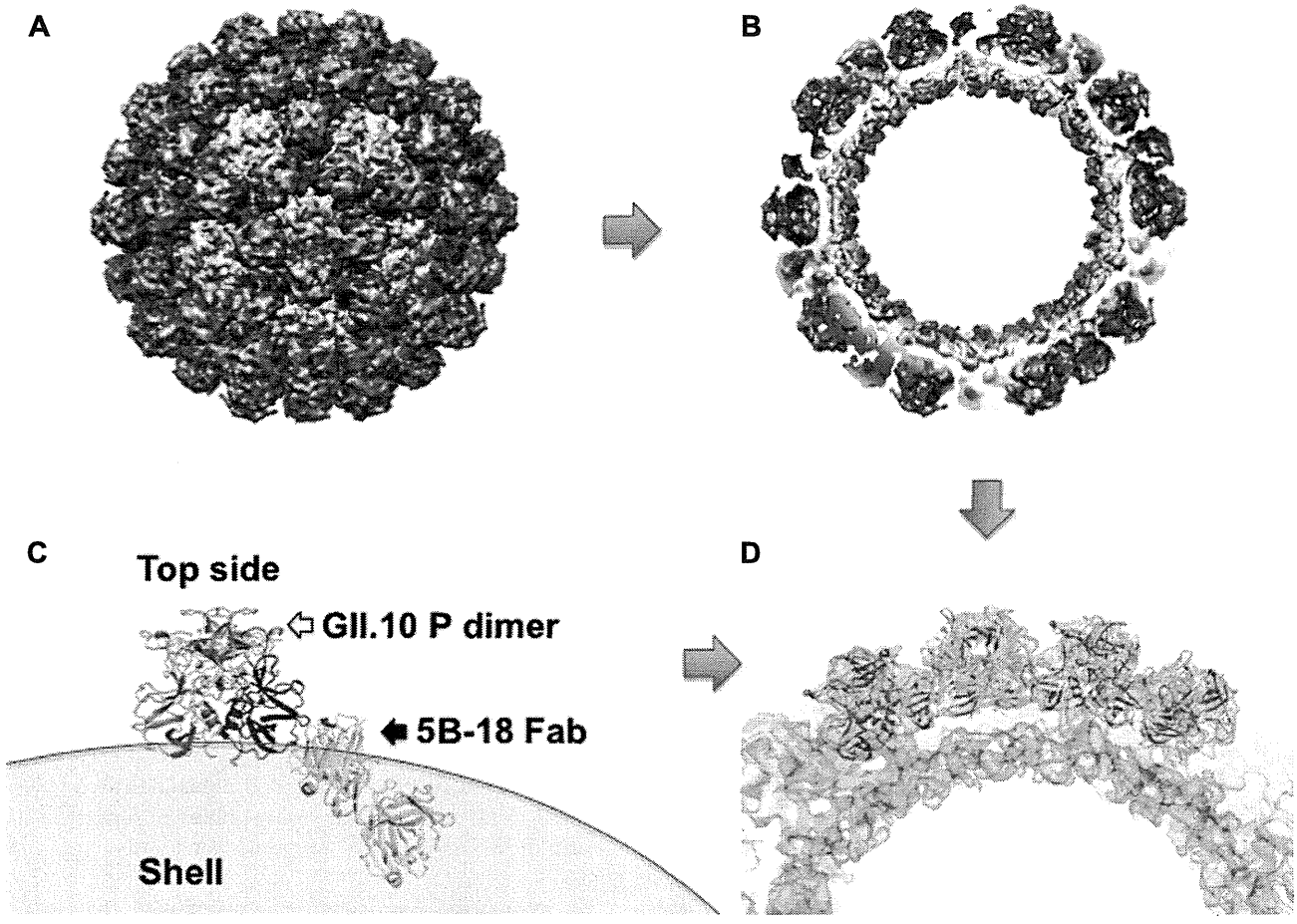

FIGURE 1 | The cryo-EM image of GII.10 VLP and the P dimer structure fit to the cryo-EM image by *in silico* modeling. The cryo-EM structure of NoV GII.10 VLP was constructed with 180 molecules of VP1 protein **(A)**. The cross-section of GII.10 VLP **(B)**. P domains (blue and green) rise up from shell domain (yellow), and it seemed to construct an outer layer of the capsid. Diagram based on the x-ray crystal structure of the GII.10 P domain-Fab complex shows Fab bound to the lower side of the P1 sub domain. Top side indicates the outside of the VLP, and the shell side contains the VLP core that is called shell. A white arrow indicates the GII.10 P dimer; the monomer is colored blue and purple. Black arrow shows MoAb 5B-18 Fab region. Green represents the heavy chain, and yellow represents the kappa chain. The part of oval shadow represents VLP shell **(C)**. The x-ray crystallography was fit into the cryo-EM structure by *in silico* modeling **(D)**. The GII.10 P domain (apo P domain structure) into the A/B dimer subunit (light blue and pink, respectively) and C/C dimer subunit (cyan).

crystallography, one of the gold standard for protein structural studies. We expressed the NoV GII.10 P domain in the *Escherichia coli* strain BL21 (DE3). The P domain was purified and stored in gel filtration buffer. Next we prepared of 5B-18 Fab fragment by immunizing a mouse with NoV GII.4-strain 445 VLPs (GenBank accession number DQ093064; Denka-Seiken, Japan). To prepare crystals of the bound complex, purified GII.10 P domain and Fab were mixed in a 1.4:1 ratio. Crystals were grown by the hanging-drop vapor-diffusion method, mixing the protein and reservoir solution (40% [vol/vol] polyethylene glycol [PEG] 400, 5% [wt/vol] PEG 3350, and 0.1 M acetic acid, pH 5.5) in a 1:1 ratio. Crystals grew over 1 week at 20°C.

One GII.10 P domain-Fab complex crystal diffracted x-rays to a resolution 3.3Å, and we solved the structure by molecular replacement with a GII.10 P domain monomer (PDB ID 3ONU) and a mouse Fab (PDB ID 1WEJ) as search models. Molecular replacement indicated an asymmetrical unit contained two P domain monomers and two 5B-18 Fabs, each with a kappa and a heavy chain (**Figure 1C**; Hansman et al., 2012).

The binding of the P domain and the Fab involved nine hydrogen bonds. Of these, eight linked the P1 subdomain to the kappa chain, and one linked the P1 subdomain and the heavy chain. More specifically, the amino acids in the P1 subdomain amino acids that interacted with the 5B-18 Fab were as follows (in each pair, the amino acids are for the P1 domain and Fab, respectively): Tyr533 and Tyr92 (one bond), Thr534 and Gly93 (three bonds), Thr534 and Trp97 (one bond), Leu535 and Tyr32 (one bond), Glu496 and Tyr92 (one bond), and Asn530 and Ser94 (one bond). Finally, Val433 and Asn52 in the heavy chain formed one hydrogen bond (Hansman et al., 2012).

CONFIRMATION OF 5B-18 BINDING

With the x-ray crystallographic analysis, we found the 5B-18 antibody bound to a hidden site on the P domain that is located inside

of the shell of NoV particle. However, in a previous study, the NoV GI structure indicated that bottom of the P domain was completely covered by the shell of NoV particle (**Figure 1C**). If the structure of GII is the same as GI, then 5B-18 could not bind GII. These results presented an apparent paradox for the 5B-18 binding mechanism. To resolve the paradox, we set out to identify the binding residue in the capsid.

From the crystallographic analysis, we knew that the 5B-18 Fab formed hydrogen bonds with residues at three sites in the P1 subdomain, called A, B, and C (**Figure 2A**). By aligning the amino acid sequences of representatives from NoV GII genotypes, we discovered that Val433 (site A) was the most variable. Other genotypes had threonine, serine, asparagine, leucine, or methionine at this position. Thr534 (site C) was mostly conserved: the only other amino acid at this position was a serine. Glu496 (site B), Asn530 (site C), Tyr533 (site C), and Leu535 (site C) were all highly conserved among the representative GII genotypes.

To confirm that 5B-18 binds the A, B, and C regions, we divided the GII.10 capsid domain into three major subdomains: N, S, P1-1 P2, and P1-2. We prepared five constructs (1–5), expressed them in an *E. coli* expression system, and identified a liner epitope of 5B-18 by western blotting (**Figure 2B**). Construct 3, a P1-2 region (i.e., A, B, and C), showed the strongest band signal, and construct 5 (i.e., B and C) showed a positive band. The intensity of the band from construct 5 was only about half the strength of construct 3 because it did not contain epitope A. However, construct 4 included only A, and constructs 1 and 2 also were not detected. Thus, the three 5B-18 epitopes A, B, and C were confirmed to be part of the binding epitope.

Next, we determined if 5B-18 binds to other NoV GII VLPs (**Figure 2A**). We prepared and purified six kinds of GII VLPs that were 809 (GII.3), 104 (GII.4), 445 (GII.6), 026 (GII.10), Hiro (GII.12), and GII.13 VLPs as aligned in **Figure 2A**. The GII VLPs that had all 5B-18 epitopes A, B, and C were captured by the anti-GII VLPs rabbit serum that was pre-coated on ELISA plate and detected with 5B-18 and horseradish peroxidase (HRP)-labeled anti-mouse IgG secondary antibodies. When the cut-off value was under 0.2, 5B-18 detected all kinds of GII VLPs in a dose-dependent manner (data not shown). These results suggested that 5B-18 binds to a variety of GII VLPs. In fact, the commercial ELISA and IC kits use 5B-18 (Denka-Seiken, Japan), and we have practical results showing that 5B-18 detects various infectious NoV GII in stool samples.

COMBINING CRYO-EM AND *IN SILICO* MODELING TO SOLVE A PARADOX

We had a simple question. Are the structures of NoV GI VLP and GII VLP the same or not? For G1 VLP, there is no space where the 5B-18 can access and bind the bottom of P domain. If the GII VLP had same conformation as the GI VLP, the lower part of the P domain would be buried under the virion shell (**Figure 1C**). However, 5B-18 binds and detects GII VLPs and GII infectious viruses. These conflicting facts suggested that the structures of the GII VLPs and infectious GII virions were different than the GI VLP structure. However, structure determinations by x-ray crystallography have many challenges and limitations, and we suspected this might be one of those cases.

To answer the question, we turned to cryo-EM and *in silico* modeling. We reconstructed the overall structure of GII.10 VLPs and 5B-18 Fabs from the x-ray structural data. To determine if the GII VLP had enough space to allow binding, we also used *in silico* modeling to fit the P and 5B-18 Fabs structures that had been derived by x-ray crystallography.

The GII.10 VLPs formed homogeneous, monodisperse particles in ice. By reference-free class averages and at 10Å resolution (0.5 FSC criterion), these icosahedral particles had several notable features, including spike-like structures extending from the vertices (**Figure 1B**), and at the three- and fivefold axes, significant amounts of the surface of the S domain were exposed (**Figure1A**). The GII.10 VLP P domain formed a second outer shell that seems to be separated from the S domain by about 15Å (**Figure 1B**). Thus, unlike the GI VLPs and virions, GII VLPs and virions seem to have a space between the shell and bottom of P domain, indicating that the two genotypes have different structures. Furthermore, the electron density was much weaker at the tip of the P domain (the P2 subdomain) than at the base. This observation is consistent with published reconstructions of calicivirus particles (Bhella et al., 2008; Bhella and Goodfellow, 2011) and indicates that the P domains have considerable heterogeneity.

Next we attempted to fit the GII.10 P domain and P domain-Fab complex structures into the GII.10 VLP cryo-EM structure. At 10Å resolution, the GII.10 P domain monomers in the VLP were easily distinguished. We manually fitted the crystal structures of the GII.10 P domain and P domain-Fab complex into the GII.10 VLP cryo-EM map, using published reports of GV.1 P domain dimers and the GV.1 cryo-EM map (Taube et al., 2010) as guides.

We refined the approximate alignment with the Fit-in-Map function in UCSF Chimera (Pettersen et al., 2004) to a cross-correlation coefficient of 0.94 (**Figure 1D**) with excellent results. The x-ray structure of the GII.10 P domain dimer (PDB ID 3ONU) unambiguously fitted the corresponding density in the cryo-EM map (**Figure 1D**). Only some loops of the P2 subdomain did not fit. They had only weak electron density, and their tips were less ordered than the S domain and P1 domains in the cryo-EM reconstruction. These subdomains are probably more flexible. P1, but not the P2, subdomains in the VLP appeared to be connected to the P domain dimers.

Next we fitted the x-ray structure of the P domain from the P domain-Fab complex into the reconstructed A/B dimer subunit and found that the 5B-18 binding site was close to an adjacent dimer of P domain (**Figure 1C**). At the twofold axes, the 5B-18 Fab was hindered by the S domain, which also provided an obstacle to assembly of the neighbor P domain dimer. However, when the P domain was fitted into the C/C dimer subunit, the 5B-18 Fab was in contact with the P domain dimer and slightly interfered with part of the S domain at the fivefold axes. Thus, the antibody binding site overlapped with part of the P1 subdomain.

Thus, this model predicted an unstable structure in which the VLP could not bind with the 5B-18 antibodies. How could this be? There are several possibilities. First, 5B-18 might bind at sites on the P domain that are only transiently exposed. Second, 5B-18 might bind to defects in the P domain. Finally, the Fab arms of 5B-18 might be very flexible.

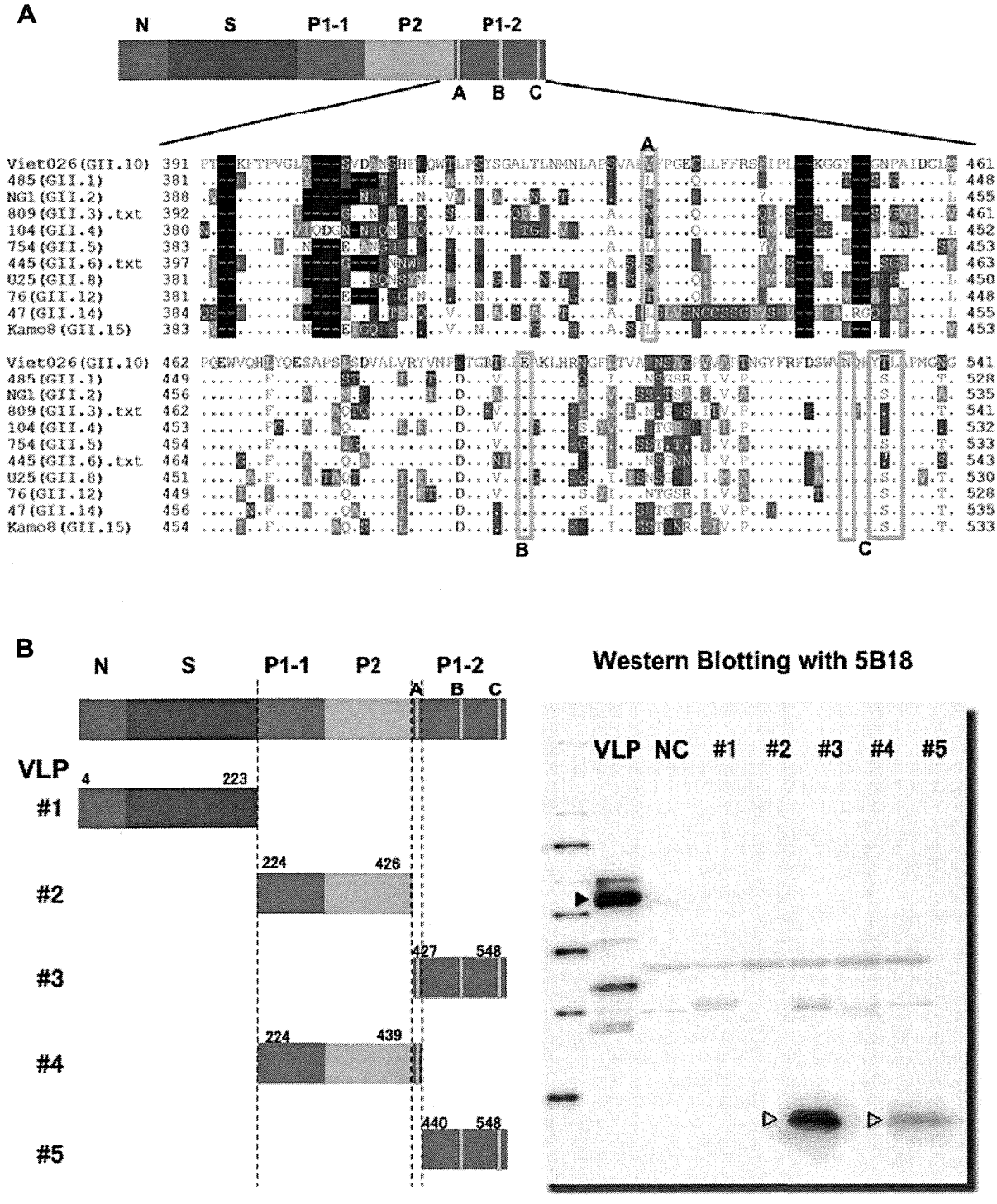

FIGURE 2 | Schematic diagram of NoV VP1 protein and the amino acid alignment of NoV GII VP1 sequences. Capsid (VP1) sequences from 11 GII genotypes were aligned, and the GII.10 capsid sequence was used as the consensus. The GII.10 P domain residues that interacted with the 5B-18 Fab involved three sites on the P domain termed A, B, and C. The six GII.10 P domain residues that interacted with the 5B-18 Fab are indicated by light blue rectangles **(A)**. Left panel of **(B)**: a schematic of the VP1 deletion mutants. The construct 1 includes the N-terminal region and shell domain of VP1, and amino acids 4–223 from the N-terminal methionine of VP1. The P1-1 and P2 domain constructs without binding site A are construct 2 (amino acids 224–426), with binding site A is construct 4 (amino acids 224–439). Construct 3 has all binding sites A, B and C (amino acids 427–548). Construct 5 deletes binding site A from construct 3 (amino acids 440–548). Right panel of **(B)**: western blotting results with 5B-18. Samples indicated as VLP, NC (negative control), mutant construct 1 (#1), #2, #3, #4 and #5. The black arrow represents VLP band at 58 kDa, and the white arrows represent #3 and #5 products at 13 kDa.

IgG flexibility is not unknown. For example, a neutralizing antibody 9C12 binds to hexon, the major coat protein of adenovirus, at a ratio of 240 antibody molecules to one virus particle or one antibody per hexon trimer (Varghese et al., 2004). By dynamic light scattering and negative-stain EM, electron-dense material coats the virus, but it was not aggregated at neutralizing ratios. In images reconstructed from cryo-EM, the viral surface was covered by electron density from the 9C12 antibody. Two Fab arms bridge two peripentonal hexons. One has a normal Fab shape and fitted the models well (Harris et al., 1998). The other arm has a somewhat distorted structure. A low-density tail extends to a third hexon that forms a minor alternate binding site. The normal arm binds to a unique site in the asymmetric unit of the virus. It has no alternate binding sites because a penton, rather than a hexon, is positioned at the icosahedral fivefold axis. In addition, the angle between the long axes of the Fabs was $<115°$ that was found in the uncomplexed IgG1 (Harris et al., 1998). Thus, flexibility is important for the bivalent binding of 9C12.

ESTIMATING THE FLEXIBILITY IN THE STRUCTURE

The findings from the 9C12 study were informative for our 5B-18 paradox. 5B-18 could reach the bottom of the P domain if the Fab domain could bend and escape the P1 subdomain or star-like structure on the shell. 5B-18 IgG bound equally well with intact and partially broken GII.10 VLPs. To determine if 5B-18 binds to intact or broken particles, we took advantage of a characteristic of norovirus VLPs: they are less stable and appear to be broken at high pHs (Ausar et al., 2006). Therefore, we looked at 5B-18 binding at different pHs. At low and neutral pHs (5.3, 6.3, and 7.3), the GII.10 VLPs were mostly homogenous in size and unbroken, but at higher pHs (8.3 and 9.3), they were less homogenous and partially broken. 5B-18 IgG bound to GII.10 VLPs at different pH values with nearly identical efficacies, regardless of the fraction of damaged particles. At pH 5.3, 6.3, and 8.3, the titer was 512,000. At pH 9.3, it was 1,024,000, and at pH 7.3, it was 2,048,000 (optical density cutoff of 0.2; Hansman et al., 2006). We also determined size distribution of the VLPs by dynamic light scattering in each pH conditions. VLPs were shown single peak on diameter 38 to 50 nm (data not shown). These results suggest that 5B-18 appears detects nominally intact GII.10 VLPs.

We studied the 5B-18 binding mechanism by x-ray crystallography, molecular virology, and cryo-EM. We combined the results in *in silico* modeling that simulates molecular dynamics and is a reliable method for revealing fluctuations in protein structure. Each technique complemented the other by filling in for data that was lacking from the others. Interestingly, the 5B-18 study suggests that VLP and viral virion have structure flexibility and that IgG molecule have flexible arms. They co-work each other and bind. *In silico* modeling is clearly a powerful tool for enhancing our understanding of basic viral processes.

ACKNOWLEDGMENTS

We thank P. Kwong and his lab members for their guidance in this work and for critical discussions about structural analysis and K. Nagayama and K. Murata for assistance with the cryo-electron microscopy and for discussions. We also thank H. Sato for giving us this great opportunity to publish our studies.

REFERENCES

Ausar, S. F., Foubert, T. R., Hudson, M. H., Vedvick, T. S., and Middaugh, C. R. (2006). Conformational stability and disassembly of Norwalk virus-like particles. Effect of pH and temperature. *J. Biol. Chem.* 281, 19478–19488.

Bhella, D., Gatherer, D., Chaudhry, Y., Pink, R., and Goodfellow, I. G. (2008). Structural insights into calicivirus attachment and uncoating. *J. Virol.* 82, 8051–8058.

Bhella, D., and Goodfellow, I. G. (2011). The cryo-electron microscopy structure of feline calicivirus bound to junctional adhesion molecule A at 9-angstrom resolution reveals receptor-induced flexibility and two distinct conformational changes in the capsid protein VP1. *J. Virol.* 85, 11381–11390.

Guix, S., Asanaka, M., Katayama, K., Crawford, S. E., Neill, F. H., Atmar, R. L., et al. (2007). Norwalk virus RNA is infectious in mammalian cells. *J. Virol.* 81, 12238–12248.

Hansman, G. S., Biertumpfel, C., Georgiev, I., McLellan, J. S., Chen, L., Zhou, T., et al. (2011). Crystal structures of GII.10 and GII.12 norovirus protruding domains in complex with histo-blood group antigens reveal details for a potential site of vulnerability. *J. Virol.* 85, 6687–6701.

Hansman, G. S., Natori, K., Shirato-Horikoshi, H., Ogawa, S., Oka, T., Katayama, K., et al. (2006). Genetic and antigenic diversity among noroviruses. *J. Gen. Virol.* 87(pt 4), 909–919.

Hansman, G. S., Taylor, D. W., McLellan, J. S., Smith, T. J., Georgiev, I., Tame, J. R., et al. (2012). Structural basis for broad detection of genogroup II noroviruses by a monoclonal antibody that binds to a site occluded in the viral particle. *J. Virol.* 86, 3635–3646.

Harris, L. J., Skaletsky, E., and McPherson, A. (1998). Crystallographic structure of an intact IgG1 monoclonal antibody. *J. Mol. Biol.* 275, 861–872.

Jiang, X., Graham, D. Y., Wang, K. N., and Estes, M. K. (1990). Norwalk virus genome cloning and characterization. *Science* 250, 1580–1583.

Jiang, X., Wang, M., Graham, D. Y., and Estes, M. K. (1992). Expression, self-assembly, and antigenicity of the Norwalk virus capsid protein. *J. Virol.* 66, 6527–6532.

Lambden, P. R., Caul, E. O., Ashley, C. R., and Clarkel, N. (1993). Sequence and genome organization of a human small round-structured (Norwalk-like) virus. *Science* 259, 516–519.

Li, X., Zhou, R., Tian, X., Li, H., and Zhou, Z. (2010). Characterization of a cross-reactive monoclonal antibody against Norovirus genogroups I, II, III and V. *Virus Res.* 151, 142–147.

Lindesmith, L. C., Beltramello, M., Donaldson, E. F., Corti, D., Swanstrom, J., Debbink, K., et al. (2012) Immunogenetic mechanisms driving norovirus GII.4 antigenic variation. *PLoS Pathog.* 8, e1002705. doi: 10.1371/journal.ppat.1002705

Pettersen, E. F., Goddard, T. D., Huang, C. C., Couch, G. S., Greenblatt, D. M., Mengm, E. C., et al. (2004). UCSF Chimera – a visualization system for exploratory research and analysis. *J. Comput. Chem.* 25, 1605–1612.

Prasad, B. V., Hardy, M. E., Dokland, T., Bella, J., Rossmann, M. G., and Estes, M. K. (1999). X-ray crystallographic structure of the Norwalk virus capsid. *Science* 286, 287–290.

Prasad, B. V., Matson, D. O., and Smith, A. W. (1994). Three-dimensional structure of calicivirus. *J. Mol. Biol.* 240, 256–64.

Taube, S., Rubin, J. R., Katpally, U., Smith, T. J., Kendall, A., Stuckey, J. A., et al. (2010). High-resolution x-ray structure and functional analysis of the murine norovirus 1 capsid protein protruding domain. *J. Virol.* 84, 5695–705.

Varghese, R., Mikyas, Y., Stewart, P. L., and Ralston, R. (2004). Postentry neutralization of adenovirus type 5 by an antihexon antibody. *J. Virol.* 78, 12320–12332.

Wobus, C. E., Thackray, L. B., and Virgin, H. W. 4th. (2006). Murine norovirus: a model system to study norovirus biology and pathogenesis. *J. Virol.* 80, 5104–5112.

Yoda, T., Suzuki, Y., Terano, Y., Yamazaki, K., Sakon, N., Kuzuguchi, T., et al. (2003). Precise characterization of norovirus (Norwalk-like virus)-specific monoclonal antibodies with broad reactivity. *J. Clin. Microbiol.* 41, 2367–2371.

Zheng, D. P., Ando, T., Fankhauser, R. L., Beard, R. S., Glass, R. I., and Monroe, S. S. (2006). Norovirus classification and proposed strain nomenclature. *Virology* 346, 312–323.

Conflict of Interest Statement: The authors declare that the research was

conducted in the absence of any commercial or financial relationships that could be construed as a potential conflict of interest.

Received: 14 August 2012; paper pending published: 24 August 2012; accepted: 18 October 2012; published online: 06 November 2012.

*Citation: Miki M and Katayama K (2012) In silico 3D structure analysis accelerates the solution of a real viral structure and antibodies docking mechanism. Front. Microbio. **3**:387. doi: 10.3389/fmicb.2012.00387*
This article was submitted to Frontiers in Virology, a specialty of Frontiers in Microbiology.